

# Practical Setting Considerations for Protective Relays That Use Incremental Quantities and Traveling Waves

Bogdan Kasztenny, Armando Guzmán, Normann Fischer,  
Mangapathirao V. Mynam, and Douglas Taylor  
*Schweitzer Engineering Laboratories, Inc.*

Published in  
*Locating Faults and Protecting Lines at the  
Speed of Light: Time-Domain Principles Applied*, 2018

Previously presented at the  
Southern African Power System Protection & Automation Conference, November 2017,  
and XIII Simposio Iberoamericano Sobre Proteccion de Sistemas  
Electricos de Potencia, February 2017

Originally presented at the  
43rd Annual Western Protective Relay Conference, October 2016

# Practical Setting Considerations for Protective Relays That Use Incremental Quantities and Traveling Waves

Bogdan Kasztenny, Armando Guzmán, Normann Fischer, Mangapathirao V. Mynam, and Douglas Taylor, *Schweitzer Engineering Laboratories, Inc.*

**Abstract**—New ultra-high-speed line protective relays that use incremental quantities and traveling waves are emerging. These relays require just a few protection settings. However, most of these settings are related to the levels of incremental quantities and propagation times of traveling waves. As such, these settings may seem new to practitioners today. This paper explains how to calculate incremental voltages and currents and how to estimate and measure traveling-wave propagation times for the purpose of configuring these protective relays. The paper reviews a number of typical settings found in incremental quantity- and traveling-wave-based protection elements and provides setting guidelines and examples for various applications, including series-compensated lines and lines with tapped loads.

## I. INTRODUCTION

Today, high-performance line protective relays include incremental quantity-based high-speed protection elements. New line protective relays are becoming available with both incremental quantity- and traveling-wave-based elements. We refer to these incremental quantity and traveling-wave (TW) protection operating principles as time-domain protection principles. One particular time-domain line protective relay uses a dedicated point-to-point fiber-optic channel to provide the first-ever TW differential protection (see Fig. 1).

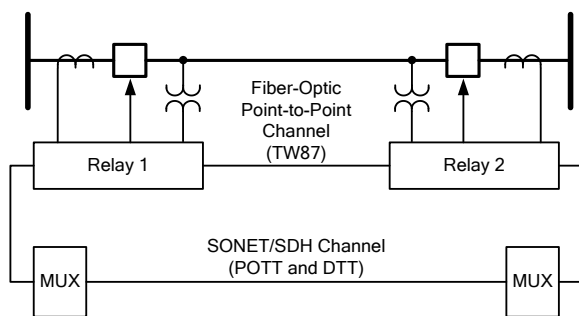


Fig. 1. Time-domain line protection application.

In addition to the TW differential (TW87) scheme, this line relay provides a communications-independent directly tripping distance element (TD21) that is based on incremental quantities as well as a permissive overreaching transfer trip (POTT) scheme. The POTT scheme uses multiplexers (MUX) to operate over a digital teleprotection channel, such as a synchronous optical network (SONET) or synchronous digital hierarchy (SDH). Alternatively, the scheme can operate over an analog channel such as power line carrier. The POTT logic uses ultra-high-speed incremental quantity (TD32) and

traveling-wave (TW32) directional elements. Fig. 2 shows a simplified diagram of this time-domain line protective relay.

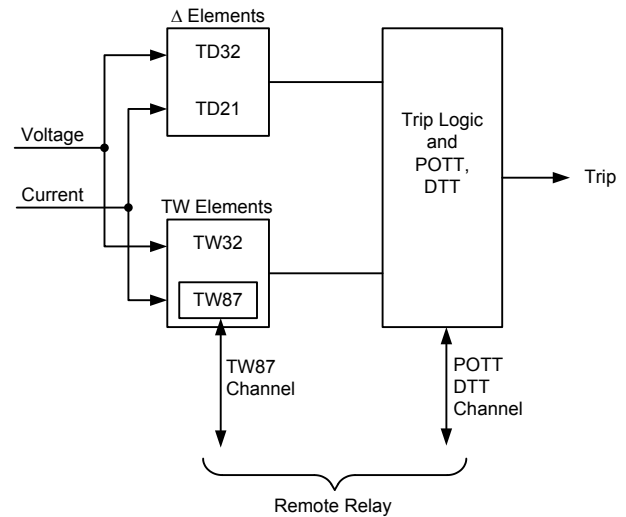


Fig. 2. Simplified diagram of a time-domain line protective relay.

Time-domain relays require only a few settings, but these settings are often critical to the relay performance. In order to achieve high speed, sensitivity, and security, these high-performing relays require accurate information about the power system in which they are applied. Relay settings provide this information and therefore they must be accurate.

We distinguish two categories of settings: nameplate data and power system-dependent data.

The nameplate data settings include items that are known and constant, and do not have to be calculated or decided upon using any engineering judgement. Instead, they just need to be retrieved from the project files. They include current transformer ratios (CTR), potential transformer ratios (PTR), line length, line impedances, system nominal frequency, nominal secondary voltage, and so on. However, all these settings shall be treated as critical protection settings. For example, a time-domain relay may adjust its low-pass filters based on the physical line length. Traditionally, line length is a noncritical fault locator setting, but the time-domain relays use every bit of information about the application to maximize performance. Assume every setting of these relays is critical.

The power system-dependent data settings are impedance and current thresholds that depend on 1) the power system short-circuit levels and 2) performance requirements of a

given application. These settings are often related to incremental voltages and currents or current TWs. These values are not directly available from the short-circuit programs commonly used by protection practitioners who set line relays.

In Section II, this paper briefly reviews the time-domain protection elements (TD32, TD21, TW32) and communications-based schemes (TW87, POTT) explaining their principles of operation, introducing their settings, and providing the rationale for the settings.

In Section III, the paper teaches about incremental quantities and explains how to calculate incremental voltages and currents using system impedances and short-circuit analysis programs.

Section IV provides setting recommendations for incremental quantity line protection elements.

Section V provides setting recommendations for TW-based line protection elements.

Section VI provides several application examples for time-domain line protection, including series-compensated and multiterminal lines.

Annex A derives the incremental replica currents and voltages used by the incremental quantity protection elements.

Annex B provides derivations for the TD32 element apparent impedance measurements and performs a worst-case error analysis of the measurements to evaluate margins required for the TD32 settings.

Annex C explains how to calculate an approximated TW propagation velocity for the purposes of setting TW-based protection elements and fault locators.

## II. TIME-DOMAIN PROTECTION ELEMENTS AND THEIR SETTINGS

This section briefly reviews the time-domain protection elements (TD32, TD21, TW32) and schemes (TW87, POTT), explaining their principles of operation. It also introduces and provides the rationale for the associated settings.

### A. Incremental Quantity Elements

These elements use incremental quantities—the differences between the instantaneous voltages and currents and their one-cycle-old values. As such, the incremental quantities contain only the fault-induced components of voltages and currents and last for one power cycle. Incremental quantity-based protection algorithms often low-pass filter the incremental quantities. This allows the relay designers to represent the protected line and system with an equivalent resistive-inductive (RL) circuit, simplifying the TD32 and TD21 operating equations. The time-domain relays typically execute the incremental quantity calculations and logic at the rate of 5–10 kHz.

#### 1) TD32 Directional Element

To realize the TD32 element, the time-domain relay calculates an incremental replica current ( $\Delta i_z$ ) as a voltage drop resulting from the incremental current ( $\Delta i$ ) at the relay location through an RL circuit with unity impedance (1  $\Omega$ ) [1]. As Fig. 3 shows, the incremental replica current is directly

proportional to the incremental voltage ( $\Delta v$ ) at the relay location. For forward faults, the incremental replica current and the incremental voltage are of opposite polarities (Fig. 3a). They are of matching polarities for reverse faults (Fig. 3b).

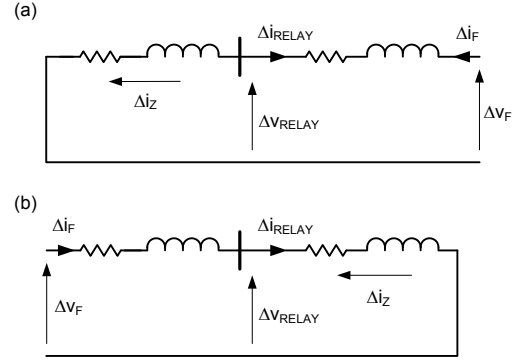


Fig. 3. TD32 directional element operating principle for forward (a) and reverse (b) faults.

When implementing the TD32 element, the time-domain line relay uses six measurement loops (three ground loops and three phase loops) to cover all fault types; calculates and integrates an operating torque; and applies adaptive thresholds for enhanced sensitivity, speed, and security [2] [3]. These adaptive forward and reverse thresholds are fractions of the expected operating torques for forward and reverse faults, respectively, and the TD32 element calculates them using the impedance threshold settings, TD32ZF and TD32ZR.

Because of the polarity relationships in Fig. 3, the sign of the operating torque changes depending on whether the fault is forward or reverse. The relay inverts the sign of the operating torque such that forward faults generate a positive torque and reverse faults generate a negative torque. For this reason, the two thresholds that the TD32 logic uses have opposite signs. The settings, however, are both positive numbers and the relay inverts the sign of the TD32ZR setting.

The time-domain relay uses the TD32 element in the POTT scheme, but the relay may also use it to supervise the TD21 protection element and, in some applications, the TW87 protection scheme. Therefore, it is critical to set the TD32ZF and TD32ZR thresholds correctly, irrespective of which time-domain protection elements are enabled and configured to trip.

#### 2) TD21 Distance Element

To realize the TD21 element, the time-domain relay calculates, as its operating signal, an instantaneous voltage change at the intended reach point using the incremental replica current, the incremental voltage, and the line RL parameters. The element tripping condition is based on the fact that the prefault voltage is the highest possible value of the voltage change at the reach point. With reference to Fig. 4, if the calculated voltage change at the reach point is higher than the prefault voltage at the reach point, the fault must be closer than the set reach,  $m_1$ . If so, the element is allowed to operate, assuming the TD32 directional element asserts forward and other security conditions are met [2] [3].

When implementing the TD21 element, the time-domain relay uses six measurement loops to cover all fault types, and it may apply an instantaneous prefault voltage at the reach point as a restraining signal for sensitivity and speed. Per common practice, the element provides independent reach settings for the phase and ground elements, TD21MP and TD21MG, respectively.

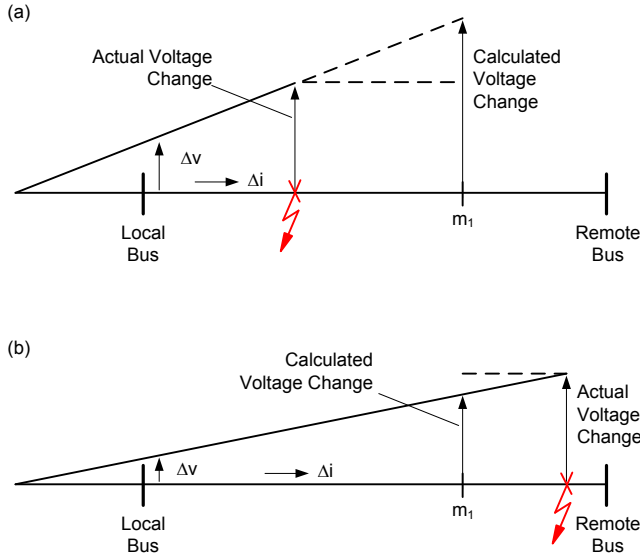


Fig. 4. TD21 underreaching element operating principle for in-zone (a) and out-of-zone (b) faults.

When using the instantaneous prefault voltage at the reach point as a restraining signal, the TD21 element must consider in-line and external series compensation (see Fig. 5). The load current ( $i$ ) causes a voltage drop across the in-line series capacitor ( $v_{SC}$ ), and this voltage drop affects the reach-point voltage ( $v_{RST}$ ). In applications with in-line series capacitors, the TD21 element calculates the voltage drop across the capacitor (Fig. 5a) and factors it into the reach point voltage calculations. However, the series capacitor may be in service or may be bypassed at any given time. The element considers both scenarios and calculates the reach point voltage with and without the series capacitor. Subsequently, it uses the higher of the two values as the TD21 restraining signal. In order to apply this solution, the relay requires the reactance of the in-line series capacitor provided by the XC setting.

When an external capacitor is present (see Fig. 5b), the TD21 element cannot calculate the voltage drop across the capacitor, because it does not measure the current through the external capacitor ( $i_{RELAY} \neq i_{SC}$ ). Therefore, when the external series capacitor is present at the remote terminal, the TD21 element uses the peak nominal voltage with margin as the restraining signal, rather than the instantaneous prefault voltage [2]. The TD21 element switches to this operating mode using the external series compensation setting, EXTSC (Y/N).

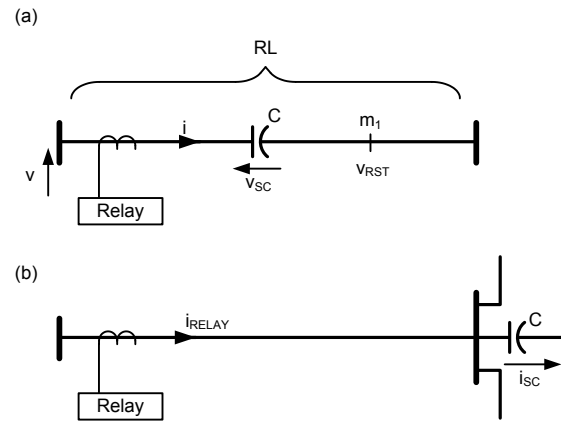


Fig. 5. Considerations for TD21 applications to lines with in-line (a) and external (b) series compensation.

### B. Traveling-Wave Elements

These elements respond to the high-frequency content (hundreds of kilohertz) in the relay input currents and, to a lesser degree, voltages. From the signal processing point of view, TWs can be understood as sharp changes in the input signals with the rise time in the order of a few microseconds. The time-domain relay samples voltages and currents at the rate of 1 MHz and extracts TWs from the raw signals using a dedicated filter. The relay may run the TW calculations every microsecond and run the TW logic every 100  $\mu$ s.

#### 1) TW32 Directional Element

The TW32 directional element compares the relative polarity of the current TWs and the voltage TWs. For a forward event, the two TWs are of opposite polarities, and for a reverse event, they are of matching polarities [1]. To realize the TW32 element, the time-domain relay integrates a torque calculated from the current and voltage TWs and checks the integrated value a few tens of microseconds into the fault (see Fig. 6) [2] [3]. As a result, the relay responds to the TW activity during the few tens of microseconds following the first TW. Once asserted, the TW32 element latches for a short period of time to act as an accelerator for the dependable TD32 directional element for permissive keying in the POTT scheme. Because of its operating principle simplicity, the TW32 element does not require settings.

When applied with coupling-capacitor voltage transformers (CCVTs), the TW32 element benefits from the parasitic capacitances across the CCVT tuning reactor and step-down transformer [2], which otherwise block the high-frequency TW signals. These capacitances create a path for these signal components, allowing some voltage TW signals to appear at the secondary CCVT terminals. The element only needs accurate polarity and timing of the first voltage TW, and therefore the element is suitable for CCVTs despite their poor reproduction of voltage TW magnitudes, especially for the second and subsequent TWs.

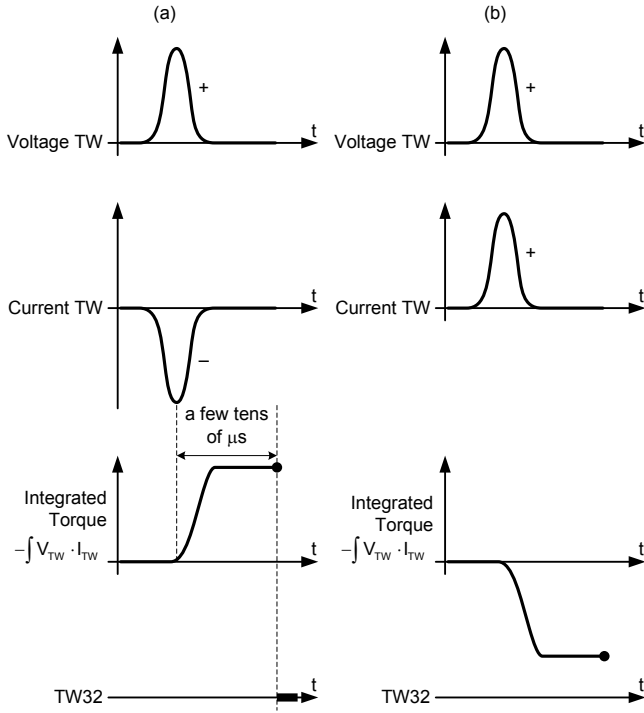


Fig. 6. Voltage and current TWs for a forward (a) and reverse (b) fault.

The TW32 element accelerates the permissive key signal in the POTT scheme and does not affect time-domain relay security. The element may not assert for faults near the voltage zero-crossing, where the change in voltage is small, or with some CCVTs. The TD32 element ensures dependability under these operating conditions.

## 2) TW87 Differential Scheme

The TW87 scheme compares time-aligned current TWs at both ends of the protected line. For an external fault, a TW that entered one terminal with a given polarity leaves the other terminal with the opposite polarity exactly after the known TW line propagation time (see Fig. 7). To realize the TW87 scheme, the time-domain relay extracts TWs from the local and remote currents and identifies the first TW for each. It then searches for the exiting TW from the local and remote currents that arrives at the opposite line terminal after the line propagation time. The relay then calculates the operating and restraining signals from the first and exiting TWs [2].

The TW87 scheme uses real-time fault-location information obtained with a double-ended fault-locating method [4]. It also uses other proprietary security conditions [2] in addition to the pickup and slope settings common in differential protection logic. The TW87 logic applies a factory-selected magnitude pickup level and security slope and provides supervision threshold settings for the user.

The supervision thresholds (TP50P and TP50G for phase and ground loops, respectively) apply to time-domain ultra-fast overcurrent elements responding to the loop incremental replica current [2]. These thresholds confirm that the in-zone event detected using TWs is actually a fault and not a switching event within the zone of protection.

In applications to series-compensated lines, the TW87 scheme is internally supervised with the TD32 element. Hence, it uses the XC and EXTSC settings to control its internal logic.

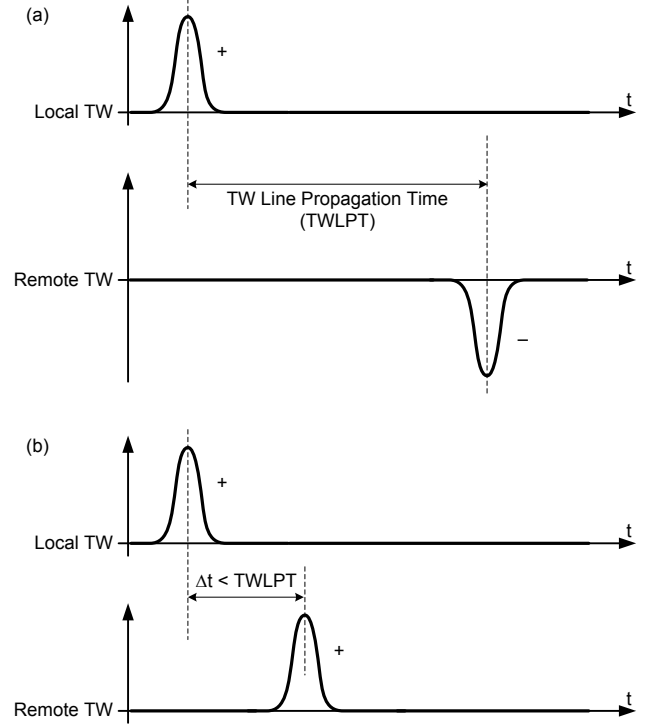


Fig. 7. Current TW timing and polarities for external (a) and internal (b) faults.

The TW line propagation time (TWLPT) is a critical TW87 scheme setting. TWLPT is the one-way TW travel time from one line terminal to the opposite terminal (see Fig. 7). This setting is critical for TW fault locating accuracy and TW87 protection scheme security. The TW87 scheme tolerates inaccuracy in the TWLPT setting of a few microseconds. Each microsecond of error in the TWLPT setting may result in a TW fault-locating error between 150 and 300 meters (500 and 1000 feet) depending on whether the relay protects cables or overhead lines. We recommend using the procedure described in Section V to measure the TWLPT value when commissioning the relay.

## C. POTT Scheme

When using the TD32 and TW32 directional elements, the POTT scheme may be susceptible to switching events within the zone of protection. Specifically, it is susceptible to bypassing of in-line series capacitors and switching (on or off) of line-side shunt reactors. These switching events change the voltage abruptly and by doing so launch TWs and introduce an incremental voltage source at the point of switching (see Fig. 8 and Fig. 9).

### 1) Bypassing In-Line Series Capacitors

With reference to Fig. 8a, the load current ( $i_{LOAD}$ ) creates a voltage drop across the capacitors ( $v_{SC}$ ). When bypassed, the capacitor becomes a source of incremental voltage connected

in series with the protected line and equivalent system impedances (Fig. 8b). This incremental voltage source drives an incremental current that circulates between the two equivalent systems and causes an incremental voltage at the relay location. The TD32 element sees such switching events with the correct directionality. If the point of switching is on the protected line, both relays correctly identify such an event as a forward event (relay incremental current and voltage have opposite polarities). The event, however, is not a fault, and the POTT scheme should not trip for it.

To address the challenge of in-zone series capacitor bypassing, the POTT scheme incorporates ultra-fast directional overcurrent supervision, similar to the TW87 scheme. The thresholds for the overcurrent supervision are TP67P and TP67G for phase and ground loops, respectively. Set these thresholds above the maximum current that flows when bypassing the capacitor, as explained in Section IV.

For lines without series compensation, set the overcurrent thresholds below the minimum fault current, determined by the desired POTT sensitivity. This process is also explained in Section IV.

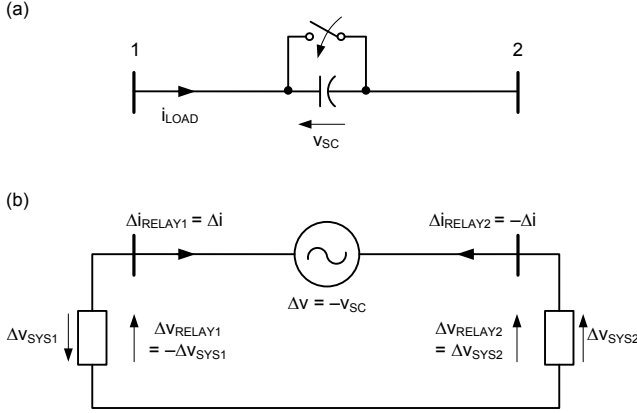


Fig. 8. Series-capacitor bypassing (a) drives incremental quantities (b).

## 2) Switching Line-Side Shunt Reactors

When a line-side shunt reactor is switched, it abruptly changes the voltage at the reactor location (Fig. 9a) and generates incremental currents and voltages at both line terminals (Fig. 9b). These incremental signals may cause the TD32 element to assert forward at both terminals. This assertion is correct because the event is on the line, in the forward direction from both relays. However, the event is not a fault and the POTT scheme should not trip for it.

In addition, when switched on, the reactor draws an inrush current with a potentially high magnitude that is difficult to calculate as a part of short-circuit studies using a standard practice. As a result, the overcurrent supervision is not a practical solution to this POTT challenge.

To address the challenge of in-zone reactor switching, we recommend removing the reactor from the protection zone by wiring the reactor current to the relay to effectively subtract it from the line current. This guideline is further explained in Section IV.

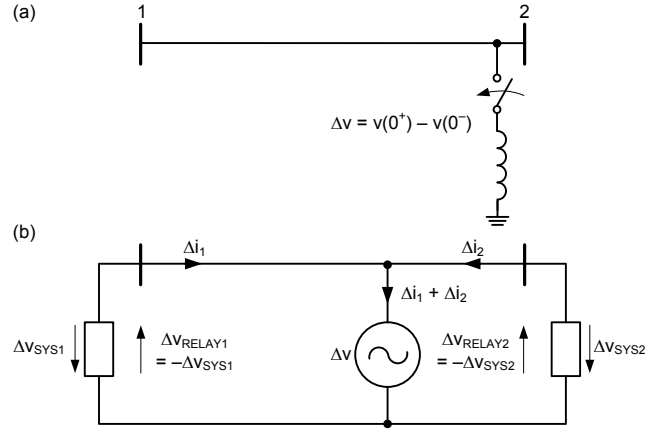


Fig. 9. Line-side reactor switching (a) generates incremental currents that may cause TD32 forward assertion at both line terminals (b).

Table I summarizes the key protection settings of the time-domain line protective relay.

TABLE I  
KEY PROTECTION SETTINGS OF THE TIME-DOMAIN LINE RELAY

Element	Setting	Description	Application
TD32	TD32ZF	Forward impedance threshold.	The TD32 logic uses these settings to derive adaptive restraining terms for forward and reverse events for fast, sensitive, and secure directional decisions.
	TD32ZR	Reverse impedance threshold.	
TD21	TD21MP	Reach for phase distance element.	The TD21 logic uses these settings to define a reach short of the remote bus, for direct tripping without the pilot channel.
	TD21MG	Reach for ground distance element.	
TW87	TWLPT	TW line propagation time.	The TW87 logic uses this setting to evaluate the time in which TWs launched by external faults that enter the protected line at one terminal, leave the line at the opposite terminal.
	TP50P	Overcurrent supervision for phase loop.	The TW87 logic uses these settings to check the event on the protected line is associated with considerable energy and therefore should be considered a fault.
	TP50G	Overcurrent supervision for ground loops.	
POTT	TP67P	Directional overcurrent supervision for phase loops.	POTT logic uses these settings to restrain on bypassing of in-line series capacitors and to select the desired sensitivity of the POTT scheme given the extremely high sensitivity of the TD32 and TW32 elements.
	TP67G	Directional overcurrent supervision for ground loops.	
General	XC	Reactance of in-line series capacitors.	TD21 logic uses these settings to modify the restraining signal.
	EXTSC	Presence (Y) or absence (N) of external series compensation.	TW87 logic uses these settings to engage extra directional supervision.

### III. INTRODUCTION TO INCREMENTAL QUANTITIES

Before discussing setting guidelines in more detail, we first review the basic theory and details behind the incremental quantity protection elements and provide examples of calculating incremental quantity currents.

#### A. Basic Theory

Together, Thevenin's theorem and the principle of superposition allow us to represent any faulted network as two separate networks, a prefault network containing only the prefault (load) voltages and currents, and a fault network containing only the fault-generated voltages and currents. The solution to the faulted network at any given time and location is the sum of the prefault and fault-generated voltages and currents. Fig. 10 illustrates this concept.

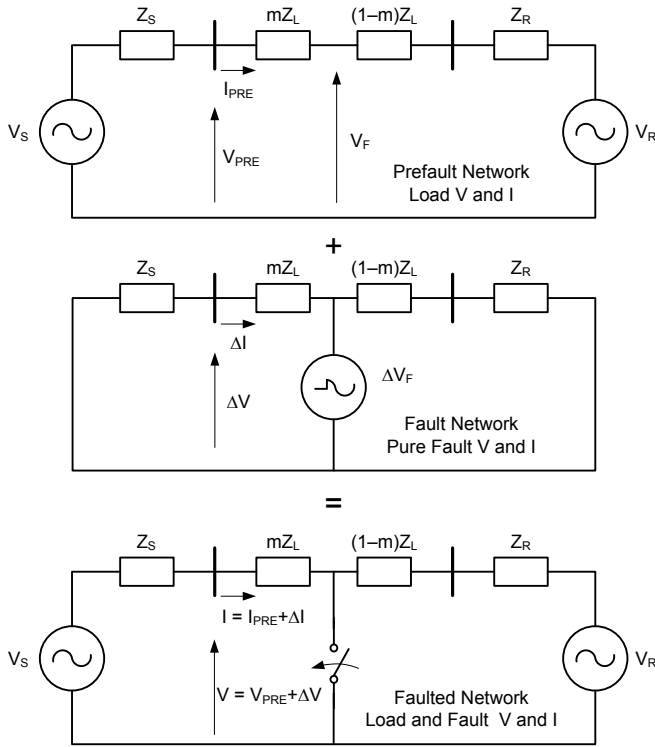


Fig. 10. Application of the superposition and Thevenin's theorems for fault analysis.

The prefault network consists of the network impedances and the Thevenin system sources that drive the system in steady state. The fault network consists of the network impedances and a single Thevenin fault source,  $\Delta V_F$ , that is equal to zero up until the fault occurs and then is equal to the negative of the Thevenin voltage at the fault location,  $V_F$ . Before the fault occurs, the fault network is not energized, and all the fault network voltages and currents are zero. When the fault occurs, the fault network experiences a transient behavior before settling into a steady state representing the fault. The incremental quantity voltages and currents reside in the fault network. Because the fault quantities are the superposition of the prefault quantities and fault-generated quantities, the relay can calculate the fault-generated (incremental) quantities as the difference between the quantities during the fault and the

prefault quantities (the latter are obtained via a delay buffer). Because the fault network quantities are differences between the fault and prefault values, we call them incremental quantities and use a  $\Delta$  symbol to represent them.

We can solve for the fault network values either in the time domain (indicated by lower-case variables in this paper) or in the frequency domain (indicated by upper-case variables). In order to speed up the protection afforded by the relay, we want to solve for the fault network values in the time domain. However, in the time domain, the voltage-current relationships are governed by differential equations and not by algebraic equations like in the frequency domain, which uses phasors. The solution to this challenge is the use of replica current, which effectively turns an RL network into an equivalent resistance-only network. Annex A first derives the incremental replica current for a single-phase circuit followed by the ground and phase loop incremental voltages and replica currents used by the incremental quantity protection elements.

For the purpose of setting calculations, it is convenient to work with loop voltages and replica currents in their phasor form. To do this, we transform the time-domain loop voltages and replica currents (see Annex A) into the frequency domain as presented in Table II.

TABLE II  
LOOP INCREMENTAL VOLTAGES AND REPLICA CURRENTS  
IN THE FREQUENCY DOMAIN

Loop	Voltage, $\Delta V$	Replica Current, $\Delta I_z$
$\Delta AG$	$\Delta V_A$	$\Delta I_A \angle Z_{iL} - \Delta I_0 \left( 1 \angle Z_{iL} - \frac{ Z_{oL} }{ Z_{iL} } \angle Z_{oL} \right)$
$\Delta BG$	$\Delta V_B$	$\Delta I_B \angle Z_{iL} - \Delta I_0 \left( 1 \angle Z_{iL} - \frac{ Z_{oL} }{ Z_{iL} } \angle Z_{oL} \right)$
$\Delta CG$	$\Delta V_C$	$\Delta I_C \angle Z_{iL} - \Delta I_0 \left( 1 \angle Z_{iL} - \frac{ Z_{oL} }{ Z_{iL} } \angle Z_{oL} \right)$
$\Delta AB$	$\Delta V_A - \Delta V_B$	$\Delta I_A \angle Z_{iL} - \Delta I_B \angle Z_{iL}$
$\Delta BC$	$\Delta V_B - \Delta V_C$	$\Delta I_B \angle Z_{iL} - \Delta I_C \angle Z_{iL}$
$\Delta CA$	$\Delta V_C - \Delta V_A$	$\Delta I_C \angle Z_{iL} - \Delta I_A \angle Z_{iL}$

Let us now look at how to calculate the incremental replica currents that a relay measures for different system faults.

#### B. Calculating Loop Incremental Replica Currents From Short-Circuit Studies

There are several short-circuit programs in common use today. While each has their unique format and features, the core components across the programs remain consistent. One consistent feature is the ability to factor in or neglect the load current in the fault calculations. Since we are interested in the incremental fault currents, we need to know the difference between the fault and prefault (load) values. One way to obtain such differences is to neglect the load in the calculations. We recognize that simply ignoring load current in the short-circuit calculations results in an inaccuracy of the calculated incremental fault current levels. When ignoring load current, the fault-point voltage in the short-circuit

calculations (e.g.,  $V_F$  in Fig. 10) is equal to the nominal system voltage rather than the true value resulting from the voltage drop along the line. However, the inaccuracy in the incremental fault current resulting from this voltage difference is typically minor.

Fig. 11 is a screenshot from the Computer-Aided Protection Engineering (CAPE<sup>®</sup>) program. We have placed an A-phase-to-ground (AG) fault at 60 percent from the NAJMA 132 kV Bus with 3 ohms of fault resistance. The program provides the A-phase and ground currents as shown in Fig. 11. Using the line data and fault currents from the program and the formulas in Table II, we can calculate the ground loop incremental replica current magnitude that the time-domain relay measures for this fault. Table III presents this system data in primary quantities.

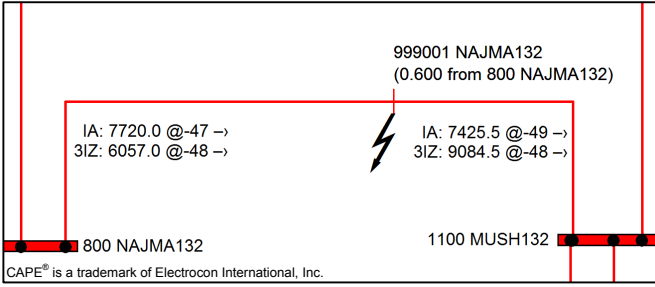


Fig. 11. CAPE image showing data for an AG fault.

TABLE III  
SYSTEM DATA IN PRIMARY QUANTITIES FOR AN AG FAULT

Line Impedance	Fault Currents
$Z_{IL} = 5.78 \angle 81.10^\circ \Omega$	$\Delta I_A = 7720.00 \angle -47.0^\circ \text{ A}$
$Z_{OL} = 15.59 \angle 82.65^\circ \Omega$	$\Delta 3I_0 = 6057.00 \angle -48.0^\circ \text{ A}$

Using a CTR of 3000/5 and a PTR of 132000/115, we convert the primary quantities to secondary quantities.

TABLE IV  
SYSTEM DATA IN SECONDARY QUANTITIES FOR AN AG FAULT

Line Impedance	Fault Current
$Z_{IL} = 3.02 \angle 81.10^\circ \Omega$	$\Delta I_A = 12.87 \angle -47.0^\circ \text{ A}$
$Z_{OL} = 8.15 \angle 82.65^\circ \Omega$	$\Delta I_0 = 3.37 \angle -48.0^\circ \text{ A}$

Note that because the relay works with zero-sequence current,  $I_0$ , we have converted the ground current,  $3I_0$ , from the short-circuit program to zero-sequence current as shown in Table IV. To calculate the replica current magnitude, we enter our system values into the ground loop replica current formula given in Table II as shown in (1).

$$|\Delta I_{ZAG}| = \left| \begin{array}{l} (12.87 \angle -47.0^\circ \text{ A}) \cdot (1 \angle 81.10^\circ) - \dots \\ (3.37 \angle -48.0^\circ \text{ A}) \cdot \left( 1 \angle 81.10^\circ - \frac{8.15}{3.02} \angle 82.65^\circ \right) \end{array} \right| \quad (1)$$

$$= 18.60 \text{ A}$$

Moving onto a multiphase fault, we simulate a bolted BC fault at the same location as that shown in Fig. 11, and the program returns the fault currents in primary quantities as shown in Table V.

TABLE V  
FAULT CURRENTS IN PRIMARY QUANTITIES FOR A BOLTED BC FAULT

B-Phase	C-Phase
$\Delta I_B = 10407.10 \angle -173.7^\circ \text{ A}$	$\Delta I_C = 10407.50 \angle 6.3^\circ \text{ A}$

Following the same procedure and using the phase loop replica current formula in Table II, gives us the replica current magnitude in secondary quantities shown in (2).

$$|\Delta I_{ZBC}| = \left| \begin{array}{l} (17.35 \angle -173.7^\circ \text{ A}) \cdot (1 \angle 81.10^\circ) - \dots \\ (17.35 \angle 6.3^\circ \text{ A}) \cdot (1 \angle 81.10^\circ) \end{array} \right| \quad (2)$$

$$= 34.70 \text{ A}$$

Let us compare these results with the exact method of factoring in the load current and calculating true incremental quantities. Assuming a pre-fault load current of 1138 A, the A-phase current for the AG fault is 8391 A and the B-phase and C-phase currents for the BC fault are 10909 A and 9816 A. When we calculate the incremental currents and use them to calculate the AG and BC replica currents, we obtain 18.10 A and 33.78 A, respectively. We see that the error for both cases is only 2.7 percent.

In general, there are two methods for obtaining the incremental currents.

- Run short-circuit studies with zero pre-fault load and use the fault currents as incremental currents.
- Run short-circuit studies with the actual pre-fault load and calculate the incremental currents as the differences between the fault currents and the pre-fault load currents (a difference between two complex numbers).

The first method is simpler but less precise. The second method involves additional calculation but is more accurate. Some short-circuit programs account for the load current and then give you the option of reporting the incremental current, simplifying the process of obtaining a more accurate result. Remember that to obtain the incremental voltages, you must always subtract the fault and pre-fault voltages as complex numbers.

To calculate overcurrent threshold settings, follow a two-step process:

1. Use the short-circuit program to obtain phase and zero-sequence incremental currents (phasors).
2. Use Table II to convert the currents into incremental replica loop currents (phasors). The relay settings typically relate to magnitudes of these loop incremental replica current phasors.

Having laid the foundation of the incremental quantity theory and how the relay calculates the loop quantities, let us move onto settings considerations for incremental quantity protection elements.

#### IV. SETTING GUIDELINES FOR INCREMENTAL QUANTITY ELEMENTS

This section focuses on setting guidelines for the incremental-quantity protection elements. We examine the

pertinent setting considerations for the TD32 element, the TD21 element, and the POTT scheme.

#### A. TD32 Settings Considerations

The TD32 element compares an operating torque against a forward and reverse adaptive restraining torque to make secure directional decisions [1]. This time-domain comparison is numerically equivalent (in the frequency domain) to comparing the apparent impedance magnitude measured by the relay against the impedance threshold settings used by the restraining signals, TD32ZF and TD32ZR. In a homogeneous system, where the system and line impedances have the same zero- to positive-sequence impedance ratios and the same positive-sequence impedance angles, the relay measures the negative of the positive-sequence impedance magnitude behind the relay during a forward fault (local source impedance). For a reverse fault, it measures the positive-sequence impedance magnitude in front of the relay (line and remote source impedance).

However, a nonhomogeneous system can result in magnitude and angle errors of the apparent impedance measurement. The amount of error in the apparent impedance dictates how we should set our impedance threshold settings for the TD32 element to operate dependably.

Annex B derives the apparent impedance measured by the relay for single-line-to-ground (SLG) and multiphase faults in both the forward and reverse directions, assuming a radial system. Equations (3) and (4) describe the loop incremental apparent impedance measured by the relay for any forward or reverse fault.

$$\Delta Z_{\text{FWD}} = -|Z_{\text{IS}}| \cdot k_{\text{ERR\_FWD}} \quad (3)$$

$$\Delta Z_{\text{REV}} = |Z_{\text{IL}} + Z_{\text{IR}}| \cdot k_{\text{ERR\_REV}} \quad (4)$$

where  $k_{\text{ERR\_FWD}}$  and  $k_{\text{ERR\_REV}}$  are complex numbers that represent the error from the ideal impedance measurement and take a different form for SLG or multiphase faults.

Annex B also provides a worst-case error analysis, assuming the largest reasonable variability in the system nonhomogeneity. For forward and reverse SLG and multiphase faults, the worst-case error terms are listed below.

$$k_{\text{MAXERR\_FSLG}} = 0.42 \angle 13.5^\circ \quad (5)$$

$$k_{\text{MAXERR\_RSLG}} = 0.71 \angle 6^\circ \quad (6)$$

$$k_{\text{MAXERR\_FMP}} = 1 \angle 10^\circ \quad (7)$$

$$k_{\text{MAXERR\_RMP}} = 1 \angle 10^\circ \quad (8)$$

The relay is designed to accommodate the maximum angle error that the nonhomogeneity introduces into the apparent impedance measurement, as Annex B explains. The magnitude error in (5) and (6) reduce the measured positive-sequence impedance for forward and reverse faults, compared with the true value. This magnitude error can result in dependability issues if we do not account for it when setting the TD32ZF and TD32ZR thresholds. Taking this analysis into consideration, we recommend the following setting guidelines for the forward and reverse impedance thresholds.

Set the forward impedance threshold, TD32ZF, to a fraction of the positive-sequence system impedance behind the relay, assuming the strongest system configuration. Use your short-circuit program to obtain the minimum local system positive-sequence impedance. If the protected line is accompanied by a parallel line, leave the parallel line in service as part of the impedance calculation. Given the worst-case analysis performed above, we recommend a dependability factor of 0.3 to account for the nonhomogeneity between the line and system impedances.

$$\text{TD32ZF} = 0.3 \cdot \text{MIN}(|Z_{\text{IS}}|) \quad (9)$$

Set the reverse impedance threshold, TD32ZR, to a fraction of the sum of the positive-sequence line impedance and the positive-sequence remote system impedance, assuming the strongest remote system configuration. A conservative option is to neglect the remote system impedance and use a dependability factor of 0.3 to account for nonhomogeneity between the line and remote system impedances.

$$\text{TD32ZR} = 0.3 \cdot |Z_{\text{IL}}| \quad (10)$$

In applications with series capacitors, if the PT is located on the bus side of the series capacitor, the series capacitor affects the TD32ZR setting. In this case,  $Z_{\text{IL}}$  in (10) should include the net impedance between the positive-sequence line impedance and the total capacitor reactance (XC).

Because the TD32 element can be used by the TD21 element and the TW87 scheme, it is important to set the TD32 impedance thresholds appropriately, regardless of whether or not TD32 is used in the POTT scheme.

#### B. TD21 Settings Considerations

Set the phase (TD21MP) and ground (TD21MG) reach in per unit (pu) of the total line impedance. The reach settings should cover most of the protected line but be set short of the remote bus with a sufficient security margin. The security margin must account for the errors of the CTs, PTs, and line impedance data, the steady-state relay errors, and the transient overreach of the TD21 element. The TD21 transient overreach is less than 10 percent [3]. The sum of the other errors is typically 10 to 15 percent. Taking all of these factors into consideration, we recommend a phase element reach setting as follows.

$$\text{TD21MP} = 0.75 \quad (11)$$

Because the zero-sequence impedance data are generally less accurate than the positive-sequence line impedance data, apply a greater security margin when setting the ground TD21 reach. The following ground element reach setting takes this inaccuracy into consideration.

$$\text{TD21MG} = 0.7 \quad (12)$$

When protecting a line with series compensation, enter the series capacitor reactance as the XC setting. We consider the compensation to be in-line when the series capacitors are located on the protected line between the line CTs and between the local relay PT and the remote bus (Fig. 12a). In a situation where the local terminal has line-side PTs and a series capacitor is in the local substation, the local terminal

does not include an in-line capacitor but the remote terminal does (Fig. 12b).

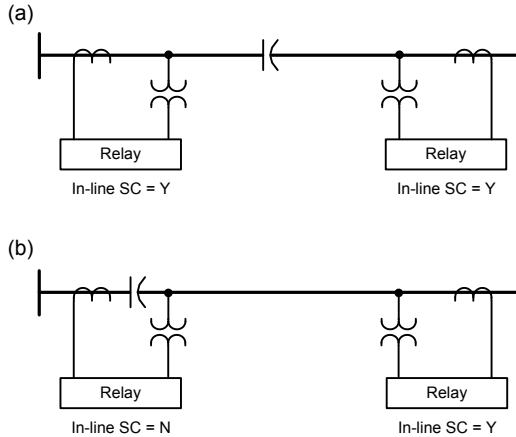


Fig. 12. Explaining the in-line series-compensation application.

For in-line capacitor applications, set the XC setting equal to the total series capacitive reactance present on the protected line. Alternatively, you can calculate XC as a product of the percentage compensation value and the secondary positive-sequence line impedance without compensation. When two or more series capacitor banks are present on the line, set XC as the sum of their reactances.

The reach settings, TD21MP and TD21MG, do not need to account for the net line and capacitor impedance, but rather can be set as a fraction of the line impedance alone. The reach settings can ignore the series capacitance because the TD21 restraining signal accounts for the effect of the in-line capacitor. Additionally, the TD21 element either restrains or trips before the operating signal is significantly affected by the fault voltage built up across the series capacitor. For this reason, the reach settings given by (11) and (12) are appropriate for lines with or without series compensation.

For applications involving external series compensation, set EXTSC = Y when the sum of the external capacitor's negative reactance and the positive inductive reactance of the line section between the remote terminal and the external capacitor is negative. If the sum is positive, do not consider the capacitor as an external capacitor for the local line terminal (EXTSC = N). Fig. 13 illustrates an example of this rule.

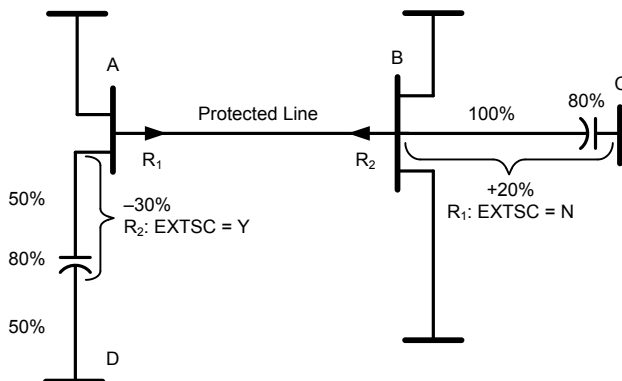


Fig. 13. Example of determining the EXTSC setting.

Note that the EXTSC setting evaluated for the bus with the  $R_2$  relay is entered as the  $R_1$  relay setting, and vice versa. When considering the EXTSC setting for Relay  $R_1$  at Terminal A, we examine the adjacent line, BC, located at the remote terminal end. Here we see that the reactance from Bus B to the capacitor bank location is a positive 20 percent, so we set EXTSC = N for Relay  $R_1$ . The setting for Relay  $R_2$  at Terminal B considers the adjacent line, AD. In this case, there is a net reactance from Bus A to the capacitor bank location equal to  $-30$  percent, so we must set EXTSC = Y for Relay  $R_2$ .

In applications where the TW87 scheme is enabled and one relay meets the external series compensation criteria, set both relays with EXTSC = Y. For example, if enabling the TW87 scheme in Relays  $R_1$  and  $R_2$  (shown in Fig. 13) set EXTSC = Y in both relays.

### C. POTT Scheme Settings Considerations

The POTT scheme is implemented using the ultra-sensitive TD32 and TW32 directional elements, which are prone to asserting for in-zone switching events. The POTT scheme uses directional overcurrent supervision in order to discern between in-zone switching events and in-zone faults. This section discusses how to appropriately set the thresholds (TP67P and TP67G) used by the overcurrent elements, given various line configurations.

#### 1) Lines Without Series Compensation

If the protected line cannot experience any in-zone switching events, then the overcurrent settings control the level of sensitivity of the POTT scheme. In this case, set TP67P and TP67G for the minimum fault current (maximum sensitivity) for an in-zone fault your utility's guidelines. For instance, consider the weakest local system impedance behind the relay and the strongest remote end system impedance. Place the fault at the end of the line and use a fault resistance as per your guidelines. For the TP67P setting, consider applying a line-to-line (LL) fault at the line end. For the TP67G setting, apply an SLG fault at the line end.

Using your short-circuit program, follow the method described in Section III to calculate the incremental phase currents for the LL fault and the incremental phase and zero-sequence currents for the SLG fault. Using the equations of Table II, convert the currents to the loop incremental replica current magnitudes for the LL and SLG faults. These current magnitudes become the settings for TP67P and TP67G, respectively. Consider a dependability margin in the range of 20 percent. Subsection VI.A provides an example of this procedure.

#### 2) Lines With Series Compensation

For series-compensated lines, TP67P and TP67G shall be set above the maximum incremental current resulting from bypassing the series capacitor. The worst-case scenario occurs for a symmetrical bypass of the capacitor. To calculate this worst-case incremental current, use the strongest system source impedance for both the local and remote line terminals. The incremental circuit modeling the symmetrical bypass is shown in Fig. 14.

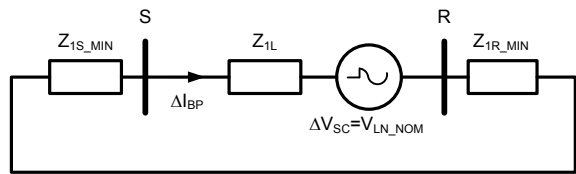


Fig. 14. Calculating worst-case incremental current during series capacitor bypassing.

Calculate the incremental current during a bypassing event by assuming that the voltage across the series capacitor is equal to the nominal line-to-neutral system voltage ( $V_{LN\_NOM}$ ) at the time of bypass. Set the TP67P and TP67G overcurrent thresholds based on the incremental current at this voltage level. In order to maximize security and sensitivity, the relay continuously calculates the voltage across the capacitor based on the load current and adapts the thresholds accordingly (Fig. 15).

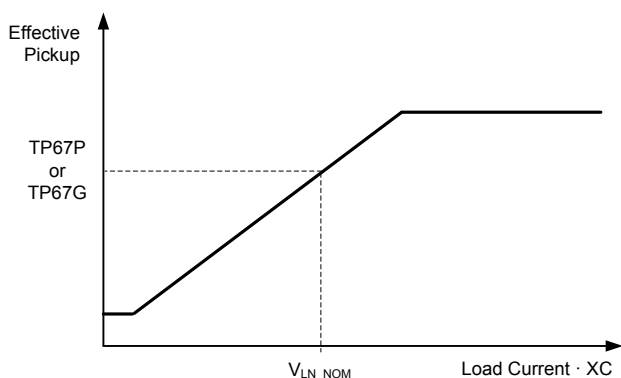


Fig. 15. Dynamic adjustment of the TP67P and TP67G thresholds in series capacitor applications.

From Fig. 14, the phase incremental current during the bypass is given by (13).

$$\Delta I_{BP} = \frac{V_{LN\_NOM}}{(Z_{IS\_MIN} + Z_{IL} + Z_{IR\_MIN})} \quad (13)$$

Since this is a balanced condition, the incremental phase currents are  $120^\circ$  out of phase. Therefore, the phase loop incremental replica current is  $\sqrt{3}$  larger than that given in (13), so set TP67P as in (14).

$$TP67P = \sqrt{3} \cdot \Delta I_{BP} \quad (14)$$

Because there is no zero-sequence current for this switching condition, the ground loop incremental replica current magnitude (see Table II) is simply equal to the value given by (13), thus set TP67G as shown in (15).

$$TP67G = \Delta I_{BP} \quad (15)$$

Consider a security margin in the range of 20 percent. Note that we are only concerned when the series capacitor is bypassed and not when it is switched into service, because the voltage across the capacitor cannot change instantaneously. Switching a capacitor into service causes much less incremental voltage than bypassing the capacitor. Subsection VI.B gives an example of performing these calculations for a series-compensated line.

### 3) In-Zone Shunt Reactors

As mentioned in Section II, the difficulty in reliably calculating inrush current when switching shunt reactors makes overcurrent supervision an impractical solution when protecting lines with reactors. Instead, we recommend removing the reactor from the POTT protection zone as Fig. 16 illustrates.

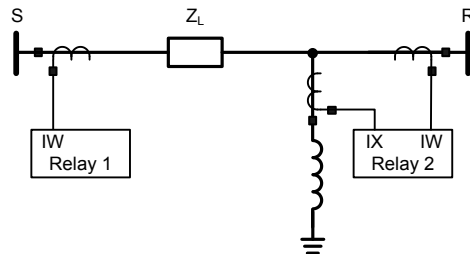


Fig. 16. Recommended application with line-side reactors that can be switched when the line is energized.

Keeping the reactor outside of the POTT zone does not prevent the incremental currents from flowing upon reactor switching. However, it ensures that during reactor switching, TD32 asserts in the reverse direction at the local relay, Relay 2, if TD32 asserts in the forward direction at the remote relay, Relay 1. With reference to Fig. 9b, the reactor current measured with the polarity convention shown in Fig. 16 is  $-(\Delta i_1 + \Delta i_2)$ , while the Relay 2 line current is  $\Delta i_2$ . The total current measured by Relay 2, as shown in Fig. 16, is therefore  $\Delta i_2 - (\Delta i_1 + \Delta i_2) = -\Delta i_1$ . This way, Relay 2 asserts in the reverse direction because it measures the incremental voltage produced by a current that is of opposite polarity with respect to the effective total current it measures. The remote Relay 1 asserts in the forward direction, but the local Relay 2 asserts in the reverse direction when the reactor is switched, securing the POTT scheme. Thus, the TP67P and TP67G thresholds can be set for sensitivity, using the procedure described in Subsection IV.C.1. If the application involves dual-breakers, externally sum the breaker CTs for wiring to one relay current input (typically, the CTs have the same ratios) and wire the reactor CT as the other relay current input (typically, the CT ratio is much smaller than the breaker CT ratios).

## V. SETTING GUIDELINES FOR THE TRAVELING-WAVE ELEMENT

We use current TWs to realize the TW87 element. The dependability of this element is based on the current TW magnitude measured at the line terminals. This magnitude ( $I_{TW}$ ) is given by (16).

$$I_{TW} = \frac{\sqrt{2} \cdot V_{SYS} \cdot \sin(POW)}{CTR \cdot (Z_C + 2 \cdot R_F)} \cdot \left( 1 + \frac{Z_C - Z_T}{Z_C + Z_T} \right) \quad (16)$$

where:

- $V_{SYS}$  = RMS voltage magnitude at the fault location for the faulted loop
- POW = point-on-wave voltage angle at fault instant
- $R_F$  = fault resistance
- $Z_C$  = line characteristic impedance
- $Z_T$  = termination characteristic impedance behind the terminal

As an example, a bolted SLG fault on an overhead line that occurs at the voltage peak on a 525 kV system results in a current of 3.2 A secondary ( $Z_C = 300 \Omega$ ,  $Z_T = 150 \Omega$ ,  $CTR = 3000/5$ ). For the same fault with  $R_F = 100 \Omega$  primary, the relay measures 1.9 A secondary. Relays equipped with TW functionality are capable of providing meaningful measurements as low as 50 mA secondary (one percent of nominal current for a 5 A nominal CT). However, for security of protection functions like TW87, a minimum required operating current is typically between 100–200 mA secondary. With appropriate security conditions built into the protection function, this minimum threshold level is factory-set to reduce application complexity.

#### A. Measuring TW Line Propagation Time

The TW87 element requires the TW line propagation time setting, TWLPT, in order to calculate a restraining quantity. The TW87 element has a built-in tolerance for error in the TWLPT setting ( $\pm 10 \mu\text{s}$ ). However, larger errors could compromise the security of the element. Therefore, it is critical to configure the relay with an accurate TWLPT value.

We recommend measuring the line propagation time using the TW recordings captured while performing a line energization test. With the remote circuit breaker open, close the local circuit breaker to energize the line. Measure the time for the wave, initiated by energizing the line, to travel to the remote line end and back again ( $2 \cdot \text{TWLPT}$ ). Use the time-domain relay TW resolution recorder to capture the currents and measure the wave propagation time. For overhead lines, you may expect the TWLPT value to be roughly the line length divided by the speed of light in free space (for underground cables, use half the speed of light). For example, a 300 km (190 mi) overhead line has a TWLPT value of about 1000  $\mu\text{s}$ .

Fig. 17 shows the TW phase currents captured by a TW fault locator during the line energization of a 161 kV, 117.11 km (72.8 mi) overhead transmission line. In this TW fault-locating application, we filtered the phase currents using an analog band-pass filter. The filter preserves the high-frequency content and rejects the fundamental frequency content. Pole scatter during energization potentially launches a separate TW in each phase, which allows for up to three independent measurements of the line propagation time. In Fig. 17, the B-phase pole closed near the voltage zero crossing resulting in an undetectable TW. Using the line length and the speed of light, we approximate the round trip travel time as shown in (17).

$$2 \cdot \text{TWLPT}_{\text{APPROX}} = \frac{2 \cdot 117.1 \text{ km}}{3 \cdot 10^8 \frac{\text{m}}{\text{s}}} = 781 \mu\text{s} \quad (17)$$

Use this time to help identify the arrival of the reflected wave from the open terminal, and then use the time stamps of the pole closure and the reflection arrival to calculate the actual round-trip time. Use half this result for the TWLPT setting. We recommend using the reflected wave from the remote open terminal associated with last pole closure. In the case of Fig. 17, this is the A-phase TW.

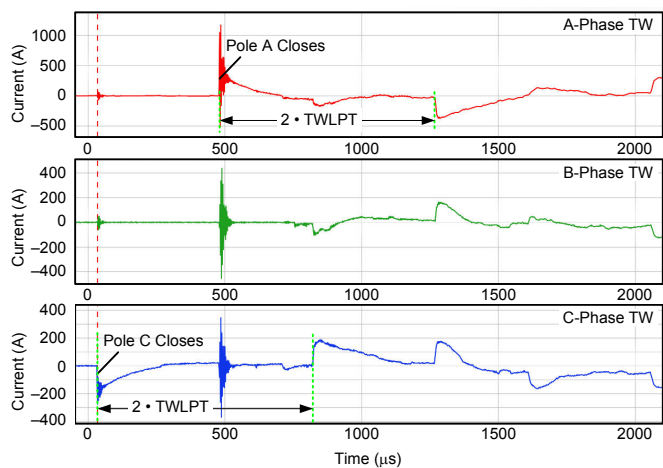


Fig. 17. Phase currents captured during line energization.

To provide the most precise measurement of the line propagation time, we recommend using tools that replicate the TW filter of the relay. Using the data recorded in Fig. 17 as our input, we plot the A-phase filtered alpha-Clarke component (see Annex C) in Fig. 18 to measure the propagation time.

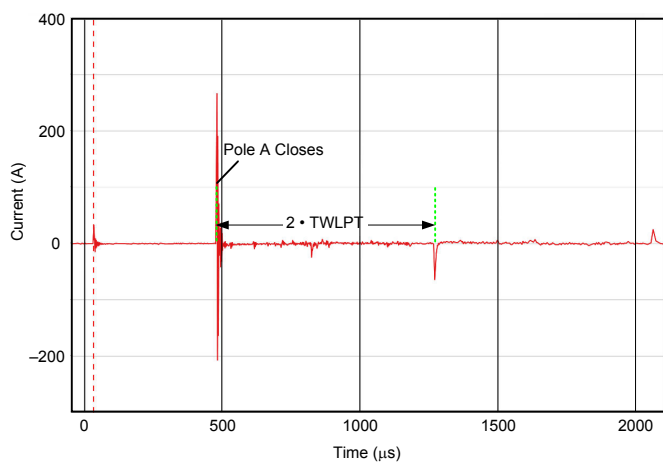


Fig. 18. A-phase filtered alpha-Clarke component.

We compute the TWLPT value as half the difference between the time when Pole A closes ( $T_{PC}$ ) and the time that the reflected wave from the remote open terminal arrives at the local end ( $T_{RW}$ ).

$$\text{TWLPT} = \frac{T_{PC} - T_{RW}}{2} = \frac{790 \mu\text{s}}{2} = 395 \mu\text{s} \quad (18)$$

Comparing (17) with (18), we see that the exact measurement in (18) was 4.5  $\mu\text{s}$  slower than the approximation. This difference is a result of the TW velocity on overhead transmission lines being slightly slower than the speed of light in free space and errors in the line length, such as line sag.

Before line energization data are available, we can approximate a value for TWLPT using line geometry data rather than the speed of light in free space. Annex C provides two options for calculating an approximated value using simulation tools.

### B. Supervisory Overcurrent Element

Similar to the POTT scheme, the TW87 scheme has a supervisory overcurrent element, which provides security for events such as switching transients and lightning strikes with no insulation break down. TP50P and TP50G define the threshold settings for overcurrent supervision of the phase and ground loops, respectively. When considering how to set these thresholds, we note that, unlike the POTT scheme, the TW87 scheme remains secure under in-line capacitor bypassing events. Bypassing the capacitive voltage in a predominately inductive system launches waves to the line terminals with opposite polarity. This causes the event to appear external to the TW87 scheme (see Fig. 7).

For this reason, we can set TP50P and TP50G for the minimum desired sensitivity, regardless of whether or not the protected line contains a series capacitor. Set TP50P and TP50G using the procedure for TP67G and TP67P as described in Subsection IV.C.1. Section VI provides examples of setting TP50P and TP50G for different line applications.

## VI. APPLICATION EXAMPLES

This section discusses how to derive relay settings for the following three examples:

- Two-terminal overhead transmission line.
- Two-terminal line with series compensation.
- Two-terminal tapped line, where the tap is not part of the line protection scheme (an unmeasured tap).

We assume the relay provides TD21, TD32, and TW87 protection as described in Section II. The examples assume a relay located at the local bus (Bus S); however, we apply the same methodology to set a relay at the remote bus (Bus R). We do not discuss nameplate type settings, such as CT and PT ratios, as these are generally well understood. The example system quantities in this section are given in secondary units (as measured by the relay), so the user can directly enter the calculated values as settings.

### A. Example 1: Two-Terminal Overhead Transmission Line

Fig. 19 shows a diagram of a two-terminal line.

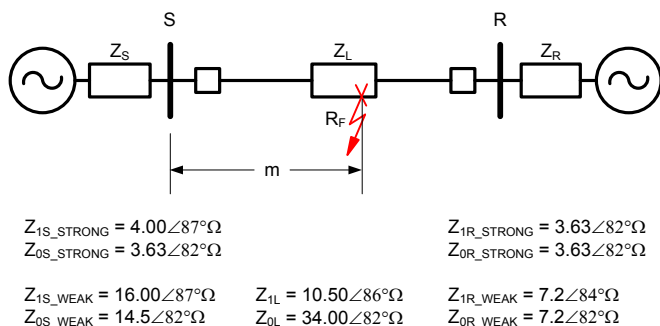


Fig. 19. Example two-terminal overhead line showing line and maximum and minimum source impedances.

For the two-source system, the Terminal S source impedance ( $Z_S$ ) represents the Thevenin equivalent impedance of the power system behind the relay. The same applies to the Terminal R source impedance.

### 1) TD32 Directional Element (TD32ZF and TD32ZR)

To determine the forward threshold value, TD32ZF, assume the strongest possible power system behind the relay such that the equivalent source impedance is the lowest, and apply an LL fault in front of the relay. Record the incremental voltages and currents, and calculate the incremental apparent impedance, the magnitude of which is equal to the positive-sequence source impedance. Using the source impedance, we can calculate the TD32ZF setting by multiplying the source impedance by the dependability factor of 0.3, according to (9). This factor accounts for any system nonhomogeneity (see Subsection IV.A). For the TD32ZR setting, multiply the line positive-sequence impedance (in ohms secondary) with the dependability factor of 0.3, according to (10).

#### Example:

Using the values shown in Fig. 19, configure the power system behind Bus S such that it has the strongest source and record the prefault voltages and currents, as shown in Table VI.

TABLE VI  
PREFault VOLTAGES AND CURRENTS AT BUS S

Voltages	Currents
$V_{A\_PRE} = 68.43 \angle 0.0^\circ$	$I_{A\_PRE} = 1.32 \angle -1.0^\circ$
$V_{B\_PRE} = 68.43 \angle -120.0^\circ$	$I_{B\_PRE} = 1.32 \angle -121.0^\circ$
$V_{C\_PRE} = 68.43 \angle 120.0^\circ$	$I_{C\_PRE} = 1.32 \angle 119.0^\circ$

The prefault currents shown in Table VI represent the load current when operating the system of Fig. 19 with a  $20^\circ$  power angle. Apply a fault in front of the relay and obtain the fault voltages and currents. In our case, we have an AB fault 10 percent down the line (i.e.,  $m = 0.1$  in Fig. 19).

TABLE VII  
FAULT VOLTAGES AND CURRENTS AT BUS S FOR AN AB FAULT

Voltages	Currents
$V_{A\_FLT} = 35.66 \angle -39.7^\circ$	$I_{A\_FLT} = 12.50 \angle -52.89^\circ$
$V_{B\_FLT} = 37.12 \angle -79.5^\circ$	$I_{B\_FLT} = 11.19 \angle 130.5^\circ$
$V_{C\_FLT} = 68.43 \angle 120.0^\circ$	$I_{C\_FLT} = 1.32 \angle 119.0^\circ$

Using the fault and prefault voltages and currents, we can calculate the incremental voltages and currents. Using these values, we calculate the phase loop incremental apparent impedance magnitude measured by the relay using (19). We note that the result of (19) is equal to the positive-sequence source impedance magnitude behind the relay.

$$|\Delta Z_{AB}| = \left| \frac{V_{AB\_FLT} - V_{AB\_PRE}}{I_{AB\_FLT} - I_{AB\_PRE}} \right| = 4.00 \Omega \quad (19)$$

where:

$$\begin{aligned} V_{AB\_FLT} &= V_{A\_FLT} - V_{B\_FLT} = 24.81 \angle 33.6^\circ \text{ V} \\ V_{AB\_PRE} &= V_{A\_PRE} - V_{B\_PRE} = 118.52 \angle 30.0^\circ \text{ V} \\ I_{AB\_FLT} &= I_{A\_FLT} - I_{B\_FLT} = 23.68 \angle -51.3^\circ \text{ A} \\ I_{AB\_PRE} &= I_{A\_PRE} - I_{B\_PRE} = 2.29 \angle 29.0^\circ \text{ A} \end{aligned}$$

We now use the value of the strongest source behind the relay to set the TD32ZF threshold, and we use the line impedance to calculate TD32ZR. We set TD32ZF and TD32ZR using a dependability factor of 0.3. Therefore, the values are as follows:

$$\text{TD32ZF} = 0.3 \cdot \text{MIN}(|Z_{IS}|) = 0.3 \cdot 4.00 \Omega = 1.20 \Omega \quad (20)$$

$$\text{TD32ZR} = 0.3 \cdot |Z_{IL}| = 0.3 \cdot 10.50 \Omega = 3.15 \Omega \quad (21)$$

Setting either TD32ZF or TD32ZR to a value greater than zero but lower than the values determined in (20) and (21) has no detrimental effect on the directional element's dependability and speed. However, for the best security, use the calculated values.

We note that an alternative option for setting TD32ZF is to use a short-circuit program to calculate the Thevenin impedance behind the relay. To perform this procedure, configure your power system for the strongest possible system behind the relay (if applicable, leave a parallel line in service), open the local breaker for the protected line, and apply an SLG fault at the local bus. The short-circuit program reports the positive-sequence Thevenin impedance that it measured for the fault. This value, multiplied by the 0.3 dependability factor, becomes the TD32ZF setting.

### 2) POTT Overcurrent Supervision (TP67G and TP67P)

In this application, no in-line switching occurs, so the supervisory overcurrent thresholds, TP67G and TP67P, can be set to the lowest possible values for maximum sensitivity. To do this, configure the power system to have the highest possible source impedance behind the relay ( $Z_{S1\_WEAK}$  and  $Z_{S0\_WEAK}$ ) and the lowest possible source impedance at the remote terminal ( $Z_{R1\_STRONG}$  and  $Z_{R0\_STRONG}$ ). This way, for forward faults, the source behind the relay contributes the lowest possible fault current. Then, simulate an SLG fault and an LL fault at the remote bus (Bus R) and record the phase and sequence quantities for these fault types. For the SLG fault, we chose to use a secondary fault resistance ( $R_F$ ) of 10  $\Omega$ . However, select the fault resistance per your utility guidelines. Using the fault currents, we can calculate the incremental replica currents for the ground and phase loops, respectively. Table VIII shows the results of applying an AG fault at Bus R.

TABLE VIII  
PREFault AND FAULT CURRENTS FOR AN AG FAULT AT BUS R

Prefault Currents	Fault Currents
$I_{A\_PRE} = 1.20 \angle 0.0^\circ$	$I_{A\_FLT} = 1.77 \angle -12.9^\circ$
$I_{B\_PRE} = 1.20 \angle -120.0^\circ$	$I_{B\_FLT} = 1.17 \angle -124.8^\circ$
$I_{C\_PRE} = 1.20 \angle 120.0^\circ$	$I_{C\_FLT} = 1.28 \angle 121.3^\circ$
$I_{0\_PRE} = 0.0 \angle 0.0^\circ$	$I_{0\_FLT} = 0.16 \angle -20.3^\circ$

Using the ground loop equations from Table II, we calculate the ground loop incremental replica current for the AG fault loop as follows.

$$\begin{aligned} \Delta I_{ZAG} &= \Delta I_A \angle Z_{IL} - \Delta I_0 \cdot \left( 1 \angle Z_{IL} - \frac{|Z_{0L}|}{|Z_{1L}|} \angle Z_{0L} \right) \\ &= 1.01 \angle 52.8^\circ \text{ A} \end{aligned} \quad (22)$$

where:

$$\Delta I_A = I_{A\_FLT} - I_{A\_PRE} = 0.66 \angle -37.0^\circ \text{ A}$$

$$\Delta I_0 = I_{0\_FLT} - I_{0\_PRE} = 0.16 \angle -20.3^\circ \text{ A}$$

From (22), we set TP67G assuming a 25-percent dependability margin as follows.

$$\text{TP67G} = 0.75 \cdot |\Delta I_{ZAG}| = 0.76 \text{ A}$$

Note that setting the pickup value to a lower value increases the sensitivity of the element, allowing the element to detect ground faults that have a higher fault resistance. For example, setting TP67G = 0.1 A allows the element to detect an SLG fault at the remote bus with an  $R_F \approx 100 \Omega$  secondary.

Table IX shows the results of applying a BC fault at Bus R.

TABLE IX  
PREFault AND FAULT CURRENTS FOR A BC FAULT AT BUS R

Prefault Currents	Fault Currents
$I_{A\_PRE} = 1.20 \angle 0.0^\circ$	$I_{A\_FLT} = 1.20 \angle 0.0^\circ$
$I_{B\_PRE} = 1.20 \angle -120.0^\circ$	$I_{B\_FLT} = 2.84 \angle -168.5^\circ$
$I_{C\_PRE} = 1.20 \angle 120.0^\circ$	$I_{C\_FLT} = 1.70 \angle 19.5^\circ$

Using the phase loop equations from Table II, we calculate the incremental replica current for the BC fault loop as shown in (23).

$$\Delta I_{ZBC} = \Delta I_B \angle Z_{IL} - \Delta I_C \angle Z_{IL} = 4.48 \angle -107.7^\circ \text{ A} \quad (23)$$

where:

$$\Delta I_B = I_{B\_FLT} - I_{B\_PRE} = 2.23 \angle 167.7^\circ \text{ A}$$

$$\Delta I_C = I_{C\_FLT} - I_{C\_PRE} = 2.25 \angle -12.1^\circ \text{ A}$$

From (23), we set TP67P assuming a 25-percent dependability margin as follows.

$$\text{TP67P} = 0.75 \cdot |\Delta I_{ZBC}| = 3.36 \text{ A}$$

### 3) TD21 Distance Element (TD21MG and TD21MP)

Considering the error sources discussed in Subsection V.B, we set the phase distance underreaching element, TP21MP, to 75 percent of the line impedance ( $Z_{1L}$ ), see (11), and the underreaching ground distance element, TP21MG, to 70 percent of the line impedance ( $Z_{1L}$ ), see (12). These reach settings are given in per unit of the line impedance. Therefore, we simply set TD21MG = 0.7 and TD21MP = 0.75 without the need for any calculations.

### 4) TW87 Differential Scheme (TP50G and TP50P)

The TW87 scheme uses the TWLPT, TP50G, and TP50P settings. For an example of how to set TWLPT, see Section V. The TP50G and TP50P threshold settings verify that the TW was launched by a fault condition and not another event such as an in-zone switching condition. In our case, we set the thresholds the same as the TP67G and TD67P settings, respectively. Therefore, we set TP50G = 0.76 A and TP50P = 3.36 A.

### B. Example 2: Two-Terminal Series-Compensated Line

For this example, we use the same simple system as shown in Fig. 19, except that the line is 80 percent series compensated ( $X_C = 8.4 \Omega$  secondary) with the capacitor located midline as shown in Fig. 20.

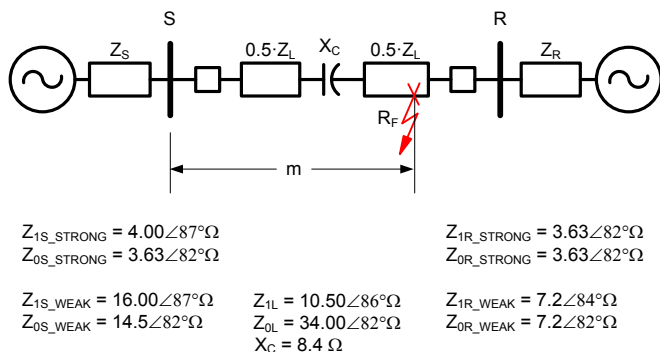


Fig. 20. Example two-terminal overhead line with midline series compensation.

#### 1) TD32 Directional Element (TD32ZF and TD32ZR)

Because the source impedance behind the relay ( $Z_S$ ) is the same as it was for the previous example, we apply the value for TD32ZF from Example 1: TD32ZF = 1.20  $\Omega$  secondary. However, because the PT is on the bus side of the series capacitor, the capacitor influences the value of TD32ZR. For any fault behind the relay at Bus S, the relay measures, at a minimum, the impedance of the line ( $Z_L$ ) modified by the series capacitor reactance ( $X_C$ ). If we ignore the source impedance behind Bus R (assume an infinite bus) and assume that the capacitor is in service, the net impedance of the line is  $Z_{IL\_NET} = (10.50 - 8.4) = 2.1 \Omega$ . Using the same dependability factor as we did in Example 1, we set TD32ZR as follows: TD32ZR = 0.3  $\cdot$   $Z_{IL\_NET} = 0.63 \Omega$ .

#### 2) POTT Overcurrent Supervision (TP67G and TP67P)

To set these overcurrent supervision elements, we follow the methodology described in Section IV. Using the strongest source behind both Bus S and Bus R and assuming nominal line-to-neutral voltage across the capacitor ( $V_{LN\_NOM}$ ), we calculate the incremental current generated from bypassing the capacitor. Fig. 21 shows the equivalent circuit to perform this calculation.

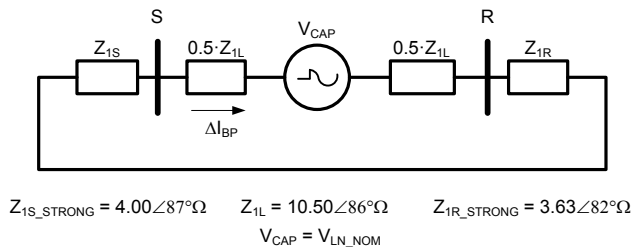


Fig. 21. Equivalent circuit to determine the incremental current during a symmetrical series capacitor bypassing operation.

First, we consider symmetrical switching (all three series capacitors bypassed simultaneously) and calculate the incremental current for each phase. Then, we calculate the incremental replica current for the ground and phase loops.

We calculate the A-phase incremental current as shown in (24).

$$\Delta I_A = \frac{V_{CAP\_A}}{Z_{1S} + Z_{1L} + Z_{1R}} = 3.81 \angle -85.4^\circ \text{A} \quad (24)$$

where:

$$V_{CAP\_A} = 69.00 \angle 0^\circ \text{V}$$

$$Z_{1S} = 4.00 \angle 87^\circ \Omega$$

$$Z_{1L} = 10.5 \angle 86^\circ \Omega$$

$$Z_{1R} = 3.63 \angle 82^\circ \Omega$$

The B-phase and C-phase incremental currents have the same current magnitudes and their angles are 120° apart. Once we have the individual phase incremental currents, we employ the equations in Table II to calculate the incremental replica currents. For the ground loops, because  $\Delta I_0$  is zero (symmetrical switching), we set TP67G equal to the magnitude of the phase incremental current according to (15), adding a 20-percent security margin as shown in (25).

$$TP67G = 1.2 \cdot 3.81 \text{A} = 4.57 \text{A} \quad (25)$$

We obtain the magnitude of the phase loop incremental replica current by multiplying the individual phase incremental currents by  $\sqrt{3}$  according to (14). We set TP67P to this value, adding a 20-percent security margin, as shown in (26).

$$TP67P = 1.2 \cdot \sqrt{3} \cdot 3.81 \text{A} = 7.92 \text{A} \quad (26)$$

Note that the relay applies the threshold values in (25) and (26) only when the voltage drop across the series capacitor equals the nominal line-to-neutral voltage. For any particular voltage drop across the series capacitor resulting from the load current, the relay adjusts the thresholds accordingly (see Fig. 15).

Next, we consider nonsymmetrical switching, where only one phase is bypassed at a time. The circuit for this is almost identical to the one shown in Fig. 21, except that now the current return path is through the system ground as shown in Fig. 22.

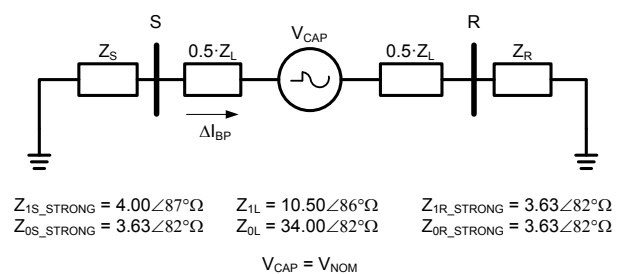


Fig. 22. Equivalent circuit to determine the incremental current during a nonsymmetrical series capacitor bypassing operation.

The incremental current for the phase loop that is bypassed is then calculated as shown in (27).

$$\Delta I_A = \frac{V_{CAP\_A}}{Z_{1\_TOTAL}(1+k0)} = 2.67 \angle -87.3^\circ \text{ A} \quad (27)$$

where:

$$V_{CAP\_A} = 69.00 \angle 0^\circ \text{ V}$$

$$Z_{1\_TOTAL} = Z_{1S} + Z_{1L} + Z_{1R} = 18.12 \angle 85.42^\circ \Omega$$

$$Z_{0\_TOTAL} = Z_{0S} + Z_{0L} + Z_{0R} = 41.26 \angle 82^\circ \Omega$$

$$k0 = \frac{Z_{0\_TOTAL} - Z_{1\_TOTAL}}{3 \cdot Z_{1\_TOTAL}} = 0.43 \angle 6.1^\circ$$

Comparing (24) and (27), we can see that a symmetrical bypass of the series capacitor bank creates the greatest incremental change in the phase currents. Therefore, to ensure security, the setting for TP69G remains as set for the symmetrical bypassing condition.

### 3) TD21 Distance Element (TD21MG and TD21MP)

When setting the TD21MG and TD21MP elements, the series capacitor does not need to be considered for the reasons explained in Subsection IV.B. Therefore, the setting values for TD21MG and TD21MP are identical to those in Example 1: TD21MG = 0.7 and TD21MP = 0.75.

### 4) Series Capacitor-Related Settings

As explained in Section IV, the relay has two settings dedicated for series-compensated lines. The first setting, XC, is the capacitive reactance of the in-line capacitor in ohms secondary. In our case, we set  $XC = 8.4 \Omega$ . The second setting, EXTSC, indicates if an external capacitor has an influence on the relay. Since we have no external series capacitors adjacent to the protected line, we set  $EXTSC = N$ .

### 5) TW87 Differential Scheme (TP50G and TP50P)

As described in Section V, the TW87 scheme needs no special consideration for series-compensated lines. For faults on the line, the series capacitor does not slow down or attenuate the TW. Because capacitor bypassing does not jeopardize the security of the TW87 scheme, the overcurrent thresholds are set the same as in Example 1: TP50G = 0.76 A and TP50P = 3.36 A.

We should consider that with the series capacitor in service, the fault currents are higher. However, the TW87 scheme has no knowledge of whether the capacitor bank is in service or not. Therefore, we can assume the bank is out of service when setting TP50G and TP50P, and ensure dependability.

For a fault in the series capacitor, we can block the TW87 scheme and allow the capacitor protection system to operate. To block the TW87 scheme, we exclude the series capacitor from the TW87 element zone by using the blocking settings (TW87BL1 and TW87BR1). Enter the distance of the series capacitor from the relay terminal, in pu, as the blocking location, TW87BL1, and enter the desired blocking radius, TW87BR1, also in pu. The series capacitor in our example is in the middle of the line; therefore, we set TW87BL1 = 0.5 pu. Assuming a two-percent security margin, we set

TW87BR1 = 0.02 pu. This way, the TW87 will not operate for faults located between 48 percent and 52 percent of the line length.

### C. Example 3: Two-Terminal Line With an Unmeasured Tap

For the tapped line example, we use the same system as in Example 1, but with a tap point at 40 percent from Bus S. The tap feeds a load via a 28 MVA, 230/24 kV delta-wye transformer. The equivalent impedance of the transformer is  $26.2 \Omega$  secondary when calculated on the transformer high-voltage (HV) side (i.e., line side). The instrument transformer ratios are PTR = 2000 and CTR = 300. Fig. 23 shows a sketch of the power system.

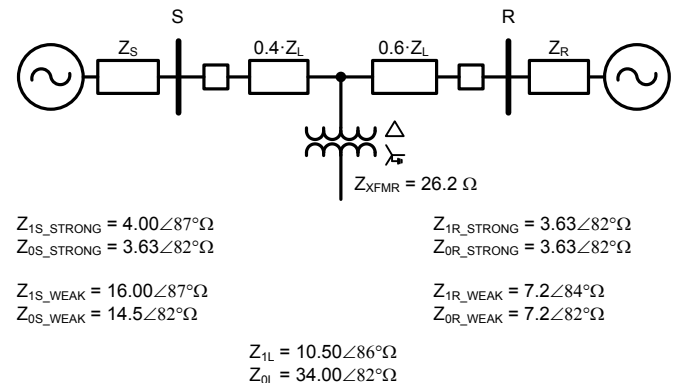


Fig. 23. Example two-terminal overhead transmission line with a transformer tap.

### 1) TD32 Directional Element (TD32ZF and TD32ZR)

The addition of the tap does not affect the TD32ZF setting, and because the tap impedance is relatively high, we do not need to change the TD32ZR setting. Therefore, we set TD32ZF = 1.20  $\Omega$  and TD32ZR = 3.15  $\Omega$ , as in Example 1.

### 2) POTT Overcurrent Supervision (TP67G and TP67P)

With an unmonitored tapped load, we do not want the POTT scheme to operate for a fault condition on the tap. Rather, we want to allow the protection at the tap point to operate. For this reason, we determine the overcurrent threshold settings based on the highest fault current supplied to the tap (we use the strongest sources behind Bus S and Bus R). To determine the TP67G setting, we place an SLG fault on the low-voltage (LV) side of the transformer. Table X shows the resulting prefault and fault current values for the Bus S relay.

The Table X fault currents appear as an LL fault due to the effect of the delta winding on the HV side of the transformer.

TABLE X  
SLG FAULT AT TRANSFORMER LV TERMINALS

Prefault Currents	Fault Currents
$I_{A\_PRE} = 1.32 \angle 0.0^\circ$	$I_{A\_FLT} = 1.52 \angle -34.0^\circ$
$I_{B\_PRE} = 1.32 \angle -120.0^\circ$	$I_{B\_FLT} = 0.96 \angle -131.2^\circ$
$I_{C\_PRE} = 1.32 \angle 120.0^\circ$	$I_{C\_FLT} = 1.69 \angle 111.9^\circ$

From Table X, we calculate the incremental currents as shown in (28).

$$\begin{aligned}\Delta I_A &= I_{A\_FLT} - I_{A\_PRE} = 0.85 \angle -94.0^\circ \text{ A} \\ \Delta I_B &= I_{B\_FLT} - I_{B\_PRE} = 0.42 \angle 86.2^\circ \text{ A} \\ \Delta I_C &= I_{C\_FLT} - I_{C\_PRE} = 0.43 \angle 86.0^\circ \text{ A}\end{aligned}\quad (28)$$

Because the delta winding of the transformer blocks any zero-sequence current flow on the HV side, the ground loop incremental replica currents are equal to the incremental phase currents given by (28). The relay uses faulted phase selection logic to enable and disable protection loops based on the maximum loop currents that it measures in addition to other security checks. The phase loop incremental replica currents for this SLG fault are shown in (29).

$$\begin{aligned}\Delta I_{ZAB} &= \Delta I_A \cdot \angle Z_{IL} - \Delta I_B \cdot \angle Z_{IL} = 1.28 \angle -8.0^\circ \text{ A} \\ \Delta I_{ZBC} &= \Delta I_B \cdot \angle Z_{IL} - \Delta I_C \cdot \angle Z_{IL} = 0.0 \angle 0.0^\circ \text{ A} \\ \Delta I_{ZCA} &= \Delta I_C \cdot \angle Z_{IL} - \Delta I_A \cdot \angle Z_{IL} = 1.28 \angle 177.2^\circ \text{ A}\end{aligned}\quad (29)$$

Comparing (28) and (29), we see that the phase loop currents are the largest, so the relay disables the ground loops, securing itself against SLG faults on the LV side of the tapped transformer. Therefore, set TP67G = 0.76 A, as in Example 1.

To determine the TP67P value, apply a three-phase fault on the LV side of the transformer. Table XI shows the resulting pre-fault and fault currents.

TABLE XI  
THREE-PHASE FAULT AT TRANSFORMER LV TERMINALS

Prefault Currents	Fault Currents
$I_{A\_PRE} = 1.32 \angle 0.0^\circ$	$I_{A\_FLT} = 1.74 \angle -44.4^\circ$
$I_{B\_PRE} = 1.32 \angle -120.0^\circ$	$I_{B\_FLT} = 1.74 \angle -164.4^\circ$
$I_{C\_PRE} = 1.32 \angle 120.0^\circ$	$I_{C\_FLT} = 1.74 \angle 75.6^\circ$

From Table XI, we calculate the incremental currents as shown in (30).

$$\begin{aligned}\Delta I_A &= I_{A\_FLT} - I_{A\_PRE} = 1.22 \angle -93.6^\circ \text{ A} \\ \Delta I_B &= I_{B\_FLT} - I_{B\_PRE} = 1.22 \angle 146.4^\circ \text{ A} \\ \Delta I_C &= I_{C\_FLT} - I_{C\_PRE} = 1.22 \angle 26.4^\circ \text{ A}\end{aligned}\quad (30)$$

Using (30), we can calculate the loop incremental replica currents for all the phase loops as shown in (31).

$$\begin{aligned}\Delta I_{ZAB} &= \Delta I_A \cdot \angle Z_{IL} - \Delta I_B \cdot \angle Z_{IL} = 2.11 \angle 22.4^\circ \text{ A} \\ \Delta I_{ZBC} &= \Delta I_B \cdot \angle Z_{IL} - \Delta I_C \cdot \angle Z_{IL} = 2.11 \angle -97.6^\circ \text{ A} \\ \Delta I_{ZCA} &= \Delta I_C \cdot \angle Z_{IL} - \Delta I_A \cdot \angle Z_{IL} = 2.11 \angle 142.4^\circ \text{ A}\end{aligned}\quad (31)$$

Therefore, a three-phase fault at the LV terminals of the tapped transformer generates a loop incremental replica current with a magnitude of 2.11 A. To prevent the POTT scheme from operating for this condition, we need to set TD67P above this value. We add a 20-percent security margin, as follows.

$$TP67P = 1.2 \cdot |\Delta I_{ZAB}| = 2.53 \text{ A} \quad (32)$$

Setting TP67P above 2.53 A does not negatively impact the security of the POTT element, but does decrease its sensitivity.

Since the tap is essentially a transformer, another factor to consider in this application is the magnitude of the inrush current once a fault on the LV side of the transformer is cleared. When the voltage magnitude recovers, it remagnetizes the transformer and the transformer draws an inrush current. The magnitude of this inrush current can be as high as 6–7 times the full load current of the transformer. In this example, the worst-case inrush current is in the order of 1.7 A. Since 1.7 A is lower than the selected TP67P threshold, the overcurrent supervision prevents the POTT scheme from operating on transformer inrush.

Should the inrush current be higher than the current for a three-phase fault on the transformer LV terminals, we can choose to increase security by using a direct transfer trip (DTT) scheme initiated by the TD21P element, rather than using the POTT scheme. However, the DTT scheme has less sensitivity for resistive LL faults than the POTT scheme. Note that we can still use the POTT scheme for ground faults because the ground loops are not as greatly impacted by transformer inrush as are the phase loops.

### 3) TD21 Distance Element (TD21MG and TD21MP)

As mentioned previously, ground faults on the LV side of the tapped transformer appear as an LL fault on the HV side of the transformer. Additionally, the tapped transformer impedance is 2.5 times the impedance of the transmission line, so if we apply the same reach settings as in the previous examples, the distance element never reaches beyond the transformer. Therefore, we can apply the TD21 reach settings used in the previous examples: TD21MG = 0.7 and TD21MP = 0.75.

### 4) TW87 Differential Scheme (TP50G and TP50P)

A fault on the LV side of the tapped transformer launches TWs toward the load and the transformer. For the TW launched toward the transformer, the transformer nearly appears as an open circuit. Most of the current TW is reflected back, and a very small part of the current TW is transmitted through the transformer via the transformer parasitic capacitance. The line terminals at Bus S and Bus R may or may not detect a TW for faults on the LV side of the transformer tap. Therefore, when setting the TP50P and TP50G thresholds, we can disregard the tap and set the thresholds as if the tap were not present: TP50G = 0.76 A and TP50P = 3.36 A, as in Example 1.

To ensure that the TW87 element does not respond to faults on the tap, we can block this region, as we did for the series capacitor in Example 2. Since the tap point is at 40 percent of the line distance from Bus S, we select TW87BL1 = 0.4 pu and, assuming a two-percent security margin, TW87BR1 = 0.02 pu.

## VII. CONCLUSIONS

New ultra-high-speed line protective relays that use incremental quantities and TWs are emerging. While highly sophisticated internally, with fast operation and security, these relays are simple to apply. The time-domain protection

elements (TD32, TD21, TW32) and schemes (TW87, POTT) require only a few settings.

The incremental quantity elements operate using the fault-generated quantities. They work with time-domain loop incremental voltages and loop incremental replica currents. We can readily calculate the settings related to these quantities using data available from short-circuit programs and line-impedance data.

The TD32 element is very sensitive, dependable, and secure and uses simple impedance thresholds as settings. The design of the TD21 element allows their reach to be set the same for lines with or without series compensation. The POTT scheme is made secure against switching events using overcurrent supervision thresholds. We set these thresholds either for sensitivity, if no in-line series compensation is present, or for security against capacitor bypassing in applications with in-line series capacitors.

The dependability of the TW87 scheme is largely based on the point-on-wave voltage angle at the fault instant. The TW87 scheme requires the TW line propagation time as a setting. We can calculate this setting using simulation tools. However, during commissioning, we recommend measuring the TW line propagation time through a line energization test. Similar to the POTT scheme, the TW87 scheme incorporates an overcurrent supervisory element. The scheme is secure for capacitor bypassing, because the TWs launched during a bypassing operation appear as an external event. For this reason, the overcurrent threshold can be set for the desired minimum fault current sensitivity.

In this paper, we have provided settings considerations for time-domain line protective relays, which we summarize in Table XII.

TABLE XII  
KEY PROTECTION SETTINGS CONSIDERATIONS OF THE TIME-DOMAIN LINE RELAY.

Element	Setting	Description	Setting Consideration
TD32	TD32ZF	Forward impedance threshold.	$0.3 \cdot \text{MIN}( Z_{IS} )$
	TD32ZR	Reverse impedance threshold.	$0.3 \cdot  Z_{IL} - XC $ Note: XC is only applicable to lines with series compensation.
TD21	TD21MP	Reach for phase distance element.	0.75 pu
	TD21MG	Reach for ground distance element.	0.7 pu

TW87	TWLPT	TW line propagation time.	Calculate an initial value using an EMTP simulation or using the speed of light in free space. Refine by measuring the propagation time in a line energization test.
	TP50P	Overcurrent supervision for phase loops.	Set for minimum desired fault current sensitivity per utility guidelines.
	TP50G	Overcurrent supervision for ground loops.	
POTT	TP67P	Directional overcurrent supervision for phase loops.	<b>No Series Compensation:</b> Set for minimum desired fault current sensitivity per utility guidelines.
	TP67G	Directional overcurrent supervision for ground loops.	<b>Series Compensation:</b> Set above maximum incremental current resulting from symmetrical series capacitor bypassing.
General	XC	Reactance of in-line series capacitors.	Set as the total series capacitive reactance present on the protected line.
	EXTSC	Presence (Y) or absence (N) of external series compensation.	Follow the guidelines of Subsection IV.B.

## VIII. ANNEX A: DERIVATION OF THE INCREMENTAL QUANTITY REPLICA CURRENT

As explained in Section IV, incremental quantity-based protection simplifies the voltage-current relationship to a resistive circuit using the concept of a replica current. This annex first derives the replica current for a single-phase circuit and then derives the loop replica currents and voltages, required for three-phase circuit protection.

### A. Single-Phase Considerations

Consider the single-phase RL time-domain network shown in Fig. 24, where a fault occurs a distance  $m$  from Terminal S. The fault network for this system is given in Fig. 25.

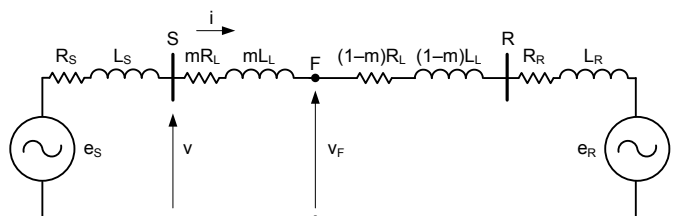


Fig. 24. Simple two-machine single-phase system with a fault at F.

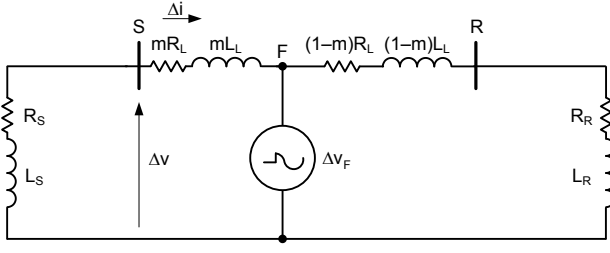


Fig. 25. Fault network of the system in Fig. 24 for analysis of incremental quantities.

At the relay location (Terminal S), the incremental voltage and current are related by a voltage drop equation across the Source S resistance and inductance.

$$\Delta v = -\left( R_s \cdot \Delta i + L_s \cdot \frac{d}{dt} \Delta i \right) \quad (33)$$

Let us scale (33) for ease of use by multiplying and dividing the right-hand side by the magnitude of the Source S impedance,  $Z_s$ .

$$\Delta v = -|Z_s| \left( \frac{R_s}{|Z_s|} \cdot \Delta i + \frac{L_s}{|Z_s|} \cdot \frac{d}{dt} \Delta i \right) \quad (34)$$

We can scale (33) without loss of generality by using a scalar. Equation (34) includes a current signal that is a combination of the instantaneous incremental current and its derivative. Let us define this current signal as with (35).

$$\Delta i_z = \frac{R_s}{|Z_s|} \cdot \Delta i + \frac{L_s}{|Z_s|} \cdot \frac{d}{dt} \Delta i = D_0 \cdot \Delta i + D_1 \cdot \frac{d}{dt} \Delta i \quad (35)$$

where:

$$D_0 = \frac{R_s}{|Z_s|} \text{ and } D_1 = \frac{L_s}{|Z_s|}$$

Now we can write a simple voltage-current equation for the incremental quantities measured at Terminal S.

$$\Delta v = -|Z_s| \cdot \Delta i_z \quad (36)$$

This derivation is valid only for an RL circuit representing the line and the source equivalent impedances. The current given by (35) is the replica current. It proportionally replicates the voltage measured at the relay location, and its naming convention ( $i_z$ , similar to the  $I \cdot Z$  product) is an indication of this. The replica current is effectively a voltage drop across an RL circuit with the gain selected to be 1 at the nominal system frequency. Equation (36) is evidence of this fact because the incremental voltage and incremental replica current are related through the source impedance magnitude. We can write the replica current (35) in a more generic form as shown in (37).

$$\Delta i_z = f_{iz}(\Delta i, R_s, L_s) = D_0(R_s, L_s) \cdot \Delta i + D_1(R_s, L_s) \cdot \frac{d}{dt} \Delta i \quad (37)$$

To transform the replica current from the time domain to the frequency domain in order to perform steady-state fault network calculations, we take the Laplace Transform of (35) as follows.

$$\Delta I_z = \frac{R_s}{|Z_s|} \cdot \Delta I + \frac{j\omega L_s}{|Z_s|} \cdot \Delta I = \frac{|Z_s| \angle Z_s}{|Z_s|} \cdot \Delta I = \Delta I \angle Z_s \quad (38)$$

### B. Three-Phase Considerations

We now expand the single-phase concept of replica current to include the proper fault loop quantities required to provide complete fault protection for three-phase power systems. Traditionally, relay designers create loop currents and voltages in such a way that the apparent impedance measured by the relay using the faulted network quantities is the positive-sequence line impedance. In the case of time-domain protection, incremental instantaneous voltage and replica current are tied with the positive-sequence line impedance magnitude.

Ground loop currents are derived assuming a bolted SLG fault on a radial system. Considering the sequence network connections for a bolted AG fault, the voltage at the relay location is given in (39).

$$V_A = Z_{1L} \cdot I_1 + Z_{1L} \cdot I_2 + Z_{0L} \cdot I_0 \quad (39)$$

We derive the loop current that results in an apparent impedance equal to the positive-sequence line impedance,  $Z_{1L}$ , as follows.

$$V_A = Z_{1L} \cdot I_1 + Z_{1L} \cdot I_2 + Z_{1L} \cdot I_0 - Z_{1L} \cdot I_0 + Z_{0L} \cdot I_0 \quad (40)$$

$$V_A = Z_{1L} \cdot I_A - (Z_{1L} - Z_{0L}) \cdot I_0 \quad (41)$$

$$V_A = Z_{1L} \cdot \left[ I_A - \left( 1 - \frac{Z_{0L}}{Z_{1L}} \right) \cdot I_0 \right] \quad (42)$$

The A-phase loop current,  $I_{AG}$ , is then the bracketed term in (42). The term in front of  $I_0$  in (42) is the familiar zero-sequence compensation factor,  $3 \cdot k_0$ . To convert the A-phase loop current into a loop replica current,  $I_{ZAG}$ , we associate the impedance angle with the current term as follows.

$$V_A = |Z_{1L}| \cdot \left[ I_A \angle Z_{1L} - \left( 1 - \frac{Z_{0L}}{Z_{1L}} \right) \cdot I_0 \angle Z_{1L} \right] \quad (43)$$

$$V_A = |Z_{1L}| \cdot I_{ZAG} \quad (44)$$

$$I_{ZAG} = I_A \angle Z_{1L} - \left( 1 - \frac{Z_{0L}}{Z_{1L}} \right) \cdot I_0 \angle Z_{1L} \quad (45)$$

In (46), we make one final alteration to the ground loop replica current to define it in terms of line impedance magnitudes and angles.

$$I_{ZAG} = I_A \angle Z_{1L} - I_0 \left( 1 \angle Z_{1L} - \frac{|Z_{0L}|}{|Z_{1L}|} \angle Z_{0L} \right) \quad (46)$$

We can now write (46) in its time-domain form invoking the function format of (37).

$$i_{ZAG} = f_{iz}(i_A, R_{1L}, L_{1L}) - \left[ f_{iz}(i_0, R_{1L}, L_{1L}) - \frac{|Z_{0L}|}{|Z_{1L}|} \cdot f_{iz}(i_0, R_{0L}, L_{0L}) \right] \quad (47)$$

The incremental form of the A-phase loop replica current simply replaces the faulted network quantities with the incremental quantities of the fault network.

$$\Delta i_{ZAG} = f_{IZ}(\Delta i_A, R_{IL}, L_{IL}) - \dots \left[ f_{IZ}(\Delta i_0, R_{IL}, L_{IL}) - \frac{|Z_{0L}|}{|Z_{1L}|} \cdot f_{IZ}(\Delta i_0, R_{0L}, L_{0L}) \right] \quad (48)$$

Turning our attention to multiphase faults, the phase loop currents and voltages are also derived in a manner to yield an apparent impedance equal to the positive-sequence line impedance. Phase loop quantities are derived assuming a bolted LL fault on a radial system. Considering the sequence network connections for a bolted BC fault, we define a Kirchoff Voltage Law (KVL) loop from the relay location to the fault point yielding (49).

$$V_1 - V_2 = Z_{1L} \cdot I_1 - Z_{1L} \cdot I_2 \quad (49)$$

The  $V_{BC}$  voltage and  $I_{BC}$  current are related to sequence voltages and currents as defined in (50) and (51), respectively.

$$\begin{aligned} V_B - V_C &= V_{BC} \\ &= (a^2 - a) \cdot V_1 - (a^2 - a) \cdot V_2 \end{aligned} \quad (50)$$

$$I_{BC} = (a^2 - a) \cdot (I_1 - I_2) \quad (51)$$

where:  $a = 1 \angle 120^\circ$

If we multiply both sides of (49) by  $(a^2 - a)$  and then make use of (50) and (51), we arrive at (52).

$$V_{BC} = Z_{1L} \cdot I_{BC} \quad (52)$$

Equation (52) contains the well-known BC phase loop voltage and current quantities and shows how they are related by the positive-sequence line impedance. Again, we convert the loop current to a loop replica current by associating the impedance angle with the current term.

$$V_{BC} = |Z_{1L}| \cdot I_{BC} \angle Z_{1L} \quad (53)$$

$$V_{BC} = |Z_{1L}| \cdot I_{ZBC} \quad (54)$$

$$I_{ZBC} = I_B \angle Z_{1L} - I_C \angle Z_{1L} \quad (55)$$

We convert the frequency domain phase loop replica current to its time-domain counterpart using the function format of (37).

$$i_{ZBC} = f_{IZ}(i_B, R_{IL}, L_{IL}) - f_{IZ}(i_C, R_{IL}, L_{IL}) \quad (56)$$

The incremental form of the BC loop replica current replaces the faulted network quantities with the incremental quantities of the fault network.

$$\Delta i_{ZBC} = f_{IZ}(\Delta i_B, R_{IL}, L_{IL}) - f_{IZ}(\Delta i_C, R_{IL}, L_{IL}) \quad (57)$$

Having solved for the loop incremental currents and voltages, we now define the following signals as the building blocks for all the phase and ground loop incremental quantities in the time domain.

$$\Delta i_0 = \frac{1}{3}(\Delta i_A + \Delta i_B + \Delta i_C) \quad (58)$$

$$\Delta i_{Z0} = f_{IZ}(\Delta i_0, R_{IL}, L_{IL}) - \frac{|Z_{0L}|}{|Z_{1L}|} \cdot f_{IZ}(\Delta i_0, R_{0L}, L_{0L}) \quad (59)$$

$$\Delta i_{ZA} = f_{IZ}(\Delta i_A, R_{IL}, L_{IL}) \quad (60)$$

$$\Delta i_{ZB} = f_{IZ}(\Delta i_B, R_{IL}, L_{IL}) \quad (61)$$

$$\Delta i_{ZC} = f_{IZ}(\Delta i_C, R_{IL}, L_{IL}) \quad (62)$$

Finally we can form the loop incremental voltages and replica currents in their time-domain format as per Table XIII.

TABLE XIII  
LOOP INCREMENTAL VOLTAGES AND REPLICA CURRENTS  
IN THE TIME DOMAIN

Loop	Voltage, $\Delta v$	Replica Current, $\Delta i_z$
$\Delta AG$	$\Delta v_A$	$\Delta i_{ZA} - \Delta i_{Z0}$
$\Delta BG$	$\Delta v_B$	$\Delta i_{ZB} - \Delta i_{Z0}$
$\Delta CG$	$\Delta v_C$	$\Delta i_{ZC} - \Delta i_{Z0}$
$\Delta AB$	$\Delta v_A - \Delta v_B$	$\Delta i_{ZA} - \Delta i_{ZB}$
$\Delta BC$	$\Delta v_B - \Delta v_C$	$\Delta i_{ZB} - \Delta i_{ZC}$
$\Delta CA$	$\Delta v_C - \Delta v_A$	$\Delta i_{ZC} - \Delta i_{ZA}$

## IX. ANNEX B: TD32 APPARENT IMPEDANCE DERIVATION

The TD32 element measures the positive-sequence impedance magnitude behind the relay for all forward faults, and the positive-sequence impedance magnitude in front of the relay for all reverse faults. This measurement deviates from the ideal impedance for nonhomogeneous systems. To quantify this deviation, this annex derives the exact impedance that the relay measures for forward or reverse faults (assuming a radial system), as the ideal result multiplied by an error term. It then analyzes the worst-case errors in the TD32 operation in order to select margins for the TD32ZF and TD32ZR settings.

### 1) Forward SLG Fault Apparent Impedance Analysis

Fig. 26 shows the incremental-sequence network connections for an SLG fault. Note that the driving voltage is not the positive-sequence system voltage but rather the negative of the fault-point voltage,  $\Delta V_F$ .

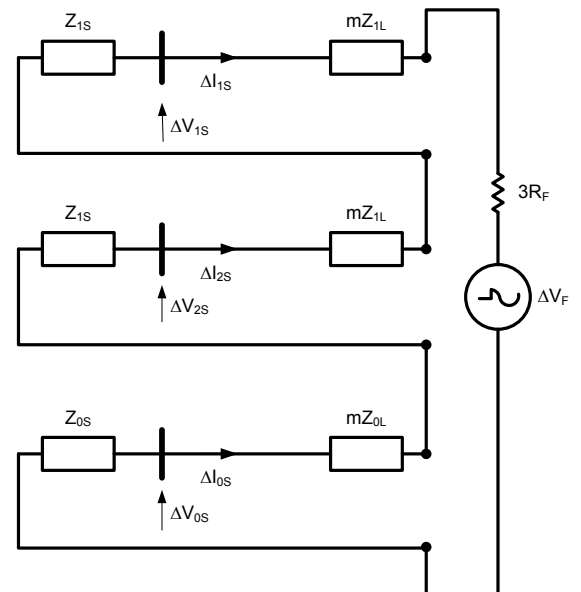


Fig. 26. Incremental-sequence network connections for a forward SLG fault.



### 3) Forward LLG Fault Apparent Impedance Analysis

Fig. 28 shows the incremental-sequence network connections for a forward LLG fault.

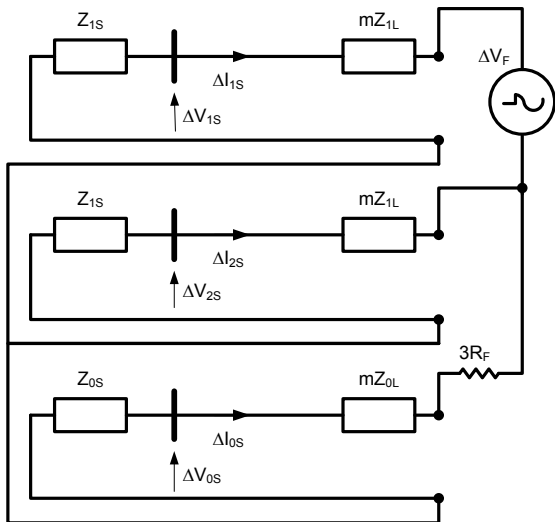


Fig. 28. Incremental-sequence network connections for a forward LLG fault.

For multiphase faults, the leading phase designation used below is the first phase that is listed in the phase loop voltage or phase loop replica current of Table II and the lagging phase designation is for the second phase. The sequence components in the following equations are written with reference to the nonfaulted phase. For example, for a BCG fault, the sequence components are referenced to the A-phase.

For a forward LLG fault, the leading and lagging incremental phase currents are given in (77) and (78) respectively. The phase loop incremental replica current is given by (79).

$$\Delta I_{\text{LEAD\_FLLG}} = a^2 \cdot \Delta I_{1S} + a \cdot \Delta I_{2S} + \Delta I_{0S} \quad (77)$$

$$\Delta I_{\text{LAG\_FLLG}} = a \cdot \Delta I_{1S} + a^2 \cdot \Delta I_{2S} + \Delta I_{0S} \quad (78)$$

$$\Delta I_{\Phi\Phi\_FLLG} = \Delta I_{\text{LEAD\_FLLG}} - \Delta I_{\text{LAG\_FLLG}} = (a^2 - a) \cdot (\Delta I_{1S} - \Delta I_{2S}) \quad (79)$$

The leading and lagging incremental phase voltages are given in (80) and (81) respectively.

$$\Delta V_{\text{LEAD\_FLLG}} = a^2 (-\Delta I_{1S} \cdot Z_{1S}) + a (-\Delta I_{2S} \cdot Z_{1S}) + (-\Delta I_{0S} \cdot Z_{0S}) \quad (80)$$

$$\Delta V_{\text{LAG\_FLLG}} = a (-\Delta I_{1S} \cdot Z_{1S}) + a^2 (-\Delta I_{2S} \cdot Z_{1S}) + (-\Delta I_{0S} \cdot Z_{0S}) \quad (81)$$

The phase loop incremental voltage is given in (82).

$$\begin{aligned} \Delta V_{\Phi\Phi\_FLLG} &= \Delta V_{\text{LEAD\_FLLG}} - \Delta V_{\text{LAG\_FLLG}} \dots \\ &= -(a^2 - a) \cdot (\Delta I_{1S} - \Delta I_{2S}) \cdot Z_{1S} \end{aligned} \quad (82)$$

Using Table II, the phase loop incremental replica current is given in (83).

$$\Delta I_{Z\Phi\Phi\_FLLG} = \Delta I_{\Phi\Phi\_FLLG} \angle Z_{1L} = (a^2 - a) \cdot (\Delta I_{1S} - \Delta I_{2S}) \angle Z_{1L} \quad (83)$$

We can now solve for the phase loop incremental apparent impedance measured by the relay by taking the ratio of (82) to (83).

$$\begin{aligned} \Delta Z_{\Phi\Phi\_FLLG} &= \frac{\Delta V_{\Phi\Phi\_FLLG}}{\Delta I_{Z\Phi\Phi\_FLLG}} = \frac{-(a^2 - a) \cdot (\Delta I_{1S} - \Delta I_{2S}) \cdot Z_{1S}}{(a^2 - a) \cdot (\Delta I_{1S} - \Delta I_{2S}) \cdot \angle Z_{1L}} \dots \\ &= -|Z_{1S}| \cdot \frac{1 \angle Z_{1S}}{1 \angle Z_{1L}} \end{aligned} \quad (84)$$

Performing similar analysis for the other multiphase faults, while assuming a radial system, produces the result given by (84). As we did with the SLG faults, we alter (84) to define the apparent impedance for a forward multiphase fault as the ideal measurement of (3) multiplied by an error term.

$$\Delta Z_{\Phi\Phi\_FMP} = -|Z_{1S}| \cdot k_{\text{ERR\_FMP}} \quad (85)$$

where:

$$k_{\text{ERR\_FMP}} = \frac{1 \angle Z_{1S}}{1 \angle Z_{1L}} \quad (86)$$

### 4) Reverse LLG Fault Apparent Impedance Analysis

Fig. 29 shows the incremental-sequence network connections for a reverse LLG fault.

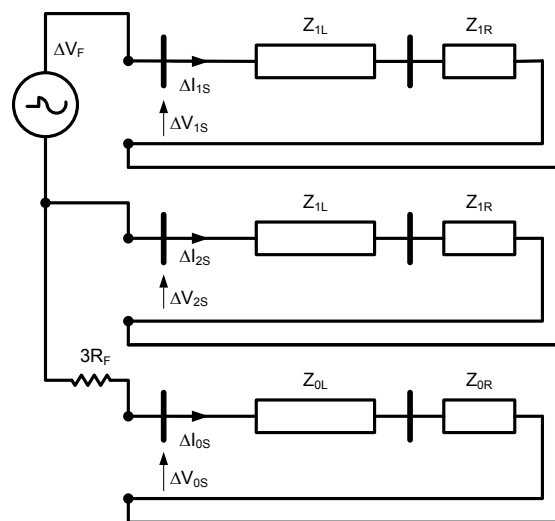


Fig. 29. Incremental-sequence network connections for a reverse LLG fault.

Following the procedure used for the forward LLG fault and referring to Fig. 29, we can calculate the phase loop incremental voltage using (87).

$$\Delta V_{\Phi\Phi\_RLLG} = (a^2 - a) \cdot (\Delta I_{1S} - \Delta I_{2S}) \cdot (Z_{1L} + Z_{1R}) \quad (87)$$

We can calculate the phase loop incremental replica current using (88).

$$\Delta I_{Z\Phi\Phi\_RLLG} = (a^2 - a) \cdot (\Delta I_{1S} - \Delta I_{2S}) \cdot \angle Z_{1L} \quad (88)$$

The phase loop incremental apparent impedance is the ratio of (87) to (88).

$$\begin{aligned} \Delta Z_{\Phi\Phi\_RLLG} &= \frac{\Delta V_{\Phi\Phi\_RLLG}}{\Delta I_{Z\Phi\Phi\_RLLG}} \\ &= \frac{(a^2 - a) \cdot (\Delta I_{1S} - \Delta I_{2S}) \cdot (Z_{1L} + Z_{1R})}{(a^2 - a) \cdot (\Delta I_{1S} - \Delta I_{2S}) \cdot \angle Z_{1L}} \end{aligned} \quad (89)$$

Equation (89) is the apparent impedance for any reverse multiphase fault, assuming a radial system. We modify (89) to

be the ideal apparent impedance of (4) multiplied by an error term.

$$\Delta Z_{\Phi\_RMP} = |Z_{1L} + Z_{1R}| \cdot k_{ERR\_RMP} \quad (90)$$

where:

$$k_{ERR\_RMP} = \frac{1 \angle (Z_{1L} + Z_{1R})}{1 \angle Z_{1L}} \quad (91)$$

### 5) Apparent Impedance Maximum Error Analysis

For a forward SLG fault, the incremental apparent impedance that the relay measures in the fault ground loop is given by (70), where the error multiplier is given by (71). From (70), we see that if the error term is equal to 1, then the apparent impedance measurement is the negative of the local source impedance magnitude as expected. From (71), we see that the system must be homogeneous for the error term to be equal to 1.

In order to determine a worst-case error, let us consider the following system conditions:

- 1)  $|Z_{0L}| = 3 \cdot |Z_{1L}|$ ,  $\theta_{0L} = \theta_{1L} - 5^\circ$
- 2)  $\theta_{1S} = \theta_{1R} = \theta_{1L} + 10^\circ$
- 3)  $|Z_{0S}| = |Z_{0R}| = 0.1 \cdot |Z_{1S}|$  to  $|Z_{0S}| = |Z_{0R}| = 3 \cdot |Z_{1S}|$
- 4)  $\theta_{0S} = \theta_{0R} = \theta_{1L} + 10^\circ$  to  $\theta_{0S} = \theta_{0R} = \theta_{1L} - 10^\circ$

Conditions 3 and Condition 4 above account for the variability in the zero-sequence source impedance depending on the presence or absence of grounding sources. Considering (71) and the variable system conditions, we see that the worst-case error occurs when the local zero-sequence source impedance is much smaller than the local positive-sequence source impedance, resulting in the following.

$$k_{MAXERR\_FSLG} = 1 \angle 10^\circ \cdot \frac{\left( 2 + \frac{0.1 \cdot |Z_{1S}| \angle 10^\circ}{|Z_{1S}|} \right)}{\left( 2 + \frac{3 \cdot |Z_{1L}| \angle -5^\circ}{|Z_{1L}|} \right)} \quad (92)$$

$$k_{MAXERR\_FSLG} = 0.42 \angle 13.5^\circ \quad (93)$$

From (93), we see that under the worst case, the relay measures an apparent impedance roughly equal to 40 percent of the local source impedance. The phase error in the apparent impedance measurement represents a fraction of the cycle (0.63 ms, assuming 60 Hz) when polarities of the incremental voltage and incremental replica current are incorrect. However, because the incremental quantities develop from zero and the relay integrates the operating and restraining torques [2] as part of making its directional decision, there is no security concern from this error.

For a reverse SLG fault, the incremental apparent impedance that the relay measures in the faulted ground loop is given by (75) and (76). If we do a worst-case analysis on (76) using the variable system conditions, we find the worst-case situation occurs when the system has a source impedance ratio (SIR) equal to one, and the remote zero-sequence source impedance is much smaller than the remote positive-sequence source impedance. Under these conditions, we can define the worst-case error with (94) and (95).

$$k_{MAXERR\_RSLG} = 1 \angle 5^\circ \cdot \frac{\left( 2 + \frac{3 \cdot |Z_{1L}| \angle -5^\circ + 0.1 \cdot |Z_{1L}| \angle 10^\circ}{|Z_{1L}| + |Z_{1L}|} \right)}{\left( 2 + \frac{3 \cdot |Z_{1L}| \angle -5^\circ}{|Z_{1L}|} \right)} \quad (94)$$

$$k_{MAXERR\_RSLG} = 0.71 \angle 6^\circ \quad (95)$$

Therefore, under the worst case, (95) indicates the relay measures an apparent impedance magnitude that is 70 percent of the sum of the positive-sequence line and remote source impedance. The phase error is less for a reverse fault compared to that of a forward fault, and results in a polarity error between the incremental voltage and incremental replica current that lasts for 0.23 ms of a 60 Hz cycle. As already stated, the security measures built into the TD32 element remove any cause for concern for this error.

When considering a multiphase fault, the apparent impedances seen by the faulted phase loop for any forward fault are given by (85) and (86), and for any reverse multiphase fault, the apparent impedances are given by (90) and (91). In the case of a forward fault, the worst-case condition of (86) is the maximum difference between the positive-sequence source and line impedance angle. A conservative estimate is a  $10^\circ$  error. Therefore,  $k_{MAXERR\_FMP} = 1 \angle 10^\circ$ . Considering a reverse fault, we find the worst-case condition of (91) to occur when the SIR is large, causing the angle error to be equal to the angle difference between the positive-sequence remote source and the line impedances. For such a situation, a  $10^\circ$  error is also a conservative choice. Therefore,  $k_{MAXERR\_RMP} = 1 \angle 10^\circ$ . As with the ground loop angle error, the security measures of the TD32 element handle this phase loop apparent impedance error.

## X. ANNEX C: TRAVELING-WAVE PROPAGATION VELOCITY CALCULATION

This section describes two methods to calculate the TW propagation velocity for estimating the TW line propagation delay. First, we briefly introduce propagation velocity and the modal transformations used for TW propagation analysis. Then, we discuss the Clarke transformation, which is necessary to analyze TWs. We follow with an example on how to calculate the line propagation velocities for a 745 kV transmission line at a particular frequency. Finally, we show an alternative approach that uses an EMTP program to model line energization and determine the TW round-trip delay. This approach provides a more realistic estimation than calculating the delay at a specific frequency.

### A. Attenuation and Propagation Velocity Theory

A fault generates surges in voltages and currents. The associated TWs attenuate as they propagate along the line because of losses caused by the line resistance and conductance.

In the analysis of a multiconductor line, the R, L, G, and C parameters of the transmission line are matrices with dimensions according to the number of conductors (n) [5]. The matrices in (96) represent the self and mutual resistance (R'),

inductance ( $L'$ ), conductance ( $G'$ ), and capacitance ( $C'$ ), in per unit of line length, for a line with three conductors.

$$\begin{aligned} \mathbf{R}' &= \begin{bmatrix} R'_{aa} & R'_{ab} & R'_{ac} \\ R'_{ba} & R'_{bb} & R'_{bc} \\ R'_{ca} & R'_{cb} & R'_{cc} \end{bmatrix} \\ \mathbf{L}' &= \begin{bmatrix} L'_{aa} & L'_{ab} & L'_{ac} \\ L'_{ba} & L'_{bb} & L'_{bc} \\ L'_{ca} & L'_{cb} & L'_{cc} \end{bmatrix} \\ \mathbf{G}' &= \begin{bmatrix} G'_{aa} & G'_{ab} & G'_{ac} \\ G'_{ba} & G'_{bb} & G'_{bc} \\ G'_{ca} & G'_{cb} & G'_{cc} \end{bmatrix} \\ \mathbf{C}' &= \begin{bmatrix} C'_{aa} & C'_{ab} & C'_{ac} \\ C'_{ba} & C'_{bb} & C'_{bc} \\ C'_{ca} & C'_{cb} & C'_{cc} \end{bmatrix} \end{aligned} \quad (96)$$

The corresponding impedance and admittance matrices, in per unit of line length are given in (97).

$$\begin{aligned} \mathbf{Z}' &= \mathbf{R}' + j\omega\mathbf{L}' \\ \mathbf{Y}' &= \mathbf{G}' + j\omega\mathbf{C}' \end{aligned} \quad (97)$$

Consider the propagation matrices  $A_v$  in (98) and  $A_i$  in (99) [6].

$$\mathbf{A}_v = \mathbf{Z}'\mathbf{Y}' \quad (98)$$

$$\mathbf{A}_i = \mathbf{Y}'\mathbf{Z}' \quad (99)$$

Our goal is to establish how the TWs propagate once they occur [7]. This is normally done using eigenvalue or modal analysis. We obtain the eigenvector matrices,  $T_i$  and  $T_v$ , so that matrix  $\Lambda$  derived in (100) and (101) takes the diagonal form in (102), meaning that the modes are decoupled; this matrix includes the eigenvalues  $\lambda_m$ .

$$\Lambda = T_v^{-1}A_vT_v \quad (100)$$

$$\Lambda = T_i^{-1}A_iT_i \quad (101)$$

$$\Lambda = \begin{pmatrix} \lambda_1 & \cdots & 0 \\ \vdots & \ddots & \vdots \\ 0 & \cdots & \lambda_n \end{pmatrix} \quad (102)$$

The square root of each eigenvalue ( $\lambda_m$ ) in  $\Lambda$  (102) represents the wave propagation constant ( $\gamma_m$ ) for the corresponding mode  $m$  as shown in (103).

$$\gamma_m = \sqrt{\lambda_m} \quad (103)$$

In (104), the real part ( $\alpha_m$ ) of the wave propagation constant ( $\gamma_m$ ) represents the attenuation constant, and the imaginary part ( $\beta_m$ ) represents the phase constant.

$$\gamma_m = \alpha_m + j\beta_m \quad (104)$$

Equation (104) has a two-fold significance. First, the nonzero value of its real part quantifies the amplitude reduction of the wave as it travels along the line. This attenuation illustrates that transmission lines have losses resulting from the resistance ( $R$ ) and conductance ( $G$ ) of the

line. Second, the nonzero value of the imaginary part in (104) is related to the propagation velocity  $v_m$  of a particular mode  $m$ , for any given frequency  $\omega$ , as defined in (105).

$$v_m = \frac{\omega}{\beta_m} \quad (105)$$

Equation (105) also shows that each mode may have unique attenuation and propagation velocity.

The above theory specifies the propagation velocity at a particular frequency. A different way to understand the dependence of the propagation velocity on frequency is to look at the steepness of the TW rising edge in the time domain. If the TW is launched as an ideal step, it contains an infinite spectrum of frequencies. The frequency components propagate at different velocities per (105), causing the initial step in the TW to become distorted. The TW edge increasingly leans the further along the line the wave travels. This phenomenon is referred to as dispersion or distortion.

### B. Clarke Component Transformation

In modal analysis, the phase signals are linear combinations of the mode signals, and vice versa. These linear combinations are expressed by the following transformation matrices.

$$\mathbf{I}_{\text{Phase}} = T_i\mathbf{I}_{\text{Mode}} \quad (106)$$

$$\mathbf{V}_{\text{Phase}} = T_v\mathbf{V}_{\text{Mode}} \quad (107)$$

$$\mathbf{I}_{\text{Mode}} = T_i^{-1}\mathbf{I}_{\text{Phase}} \quad (108)$$

$$\mathbf{V}_{\text{Mode}} = T_v^{-1}\mathbf{V}_{\text{Phase}} \quad (109)$$

We use the Clarke transformation [8] for obtaining decoupled modal currents and simplifying the study of TW propagation for protection and faulted-phase selection. Equation (110) defines the Clarke components of the instantaneous phase currents, with reference to the A-phase.

$$\begin{bmatrix} i_0 \\ i_\alpha \\ i_\beta \end{bmatrix} = T_c^{-1} \begin{bmatrix} i_A \\ i_B \\ i_C \end{bmatrix} = \frac{1}{3} \begin{bmatrix} 1 & 1 & 1 \\ 2 & -1 & -1 \\ 0 & \sqrt{3} & -\sqrt{3} \end{bmatrix} \begin{bmatrix} i_A \\ i_B \\ i_C \end{bmatrix} \quad (110)$$

The three modes are referred to as zero, alpha, and beta. If equal currents flow down the A, B, and C conductors and return in the earth, then only the zero mode, shown in the top row of (110), is excited. If all of the current flows down the A-phase and half returns on the B-phase and C-phase, then only the alpha mode is excited, shown in the middle row of (110). If all the current flows down the B-phase and returns on C-phase, then only the beta mode is excited.

The Clarke components calculated with reference to the A-phase work well for AG and BC faults but do not work optimally for other fault types.

In order to cover all fault types, we can use three sets of Clarke components with reference to the A-phase, B-phase, and C-phase, as follows:

$$\begin{bmatrix} i_\alpha^A \\ i_\beta^A \\ i_0^A \end{bmatrix} = \frac{1}{3} \begin{bmatrix} 2 & -1 & -1 \\ 0 & \sqrt{3} & -\sqrt{3} \\ 1 & 1 & 1 \end{bmatrix} \begin{bmatrix} i_A \\ i_B \\ i_C \end{bmatrix} \quad (111)$$

$$\begin{bmatrix} i_{\alpha}^B \\ i_{\beta}^B \\ i_{0}^B \end{bmatrix} = \frac{1}{3} \begin{bmatrix} -1 & 2 & -1 \\ -\sqrt{3} & 0 & \sqrt{3} \\ 1 & 1 & 1 \end{bmatrix} \begin{bmatrix} i_A \\ i_B \\ i_C \end{bmatrix} \quad (112)$$

$$\begin{bmatrix} i_{\alpha}^C \\ i_{\beta}^C \\ i_{0}^C \end{bmatrix} = \frac{1}{3} \begin{bmatrix} -1 & -1 & 2 \\ \sqrt{3} & -\sqrt{3} & 0 \\ 1 & 1 & 1 \end{bmatrix} \begin{bmatrix} i_A \\ i_B \\ i_C \end{bmatrix} \quad (113)$$

The alpha components are appropriate for analyzing TWs launched by SLG and three-phase faults. The beta components are appropriate for analyzing TWs launched by LL faults.

C. Calculating Propagation Velocity at a Specific Frequency

We use the line/cable constant (LCC) program, included in ATPDraw™, to calculate the propagation delay and wave velocities of a 193 km (120 mi), 745 kV transmission line. The ac resistances of the phase conductors and shield wires are 0.0201 and 3.75 ohms/mile, respectively. We assume a ground resistivity of 100 ohms/meter. Fig. 30 shows the line tower and conductor configuration.

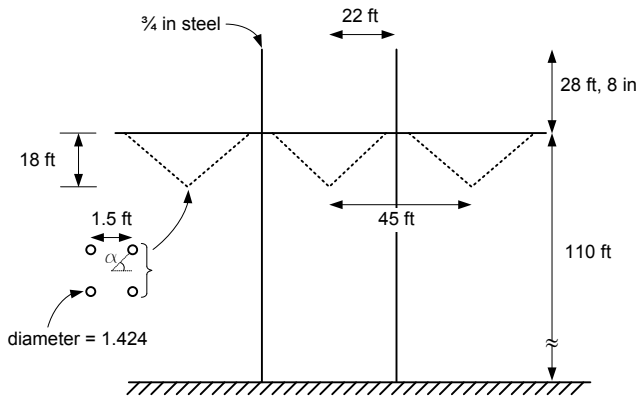


Fig. 30. Tower and conductor configuration of a 745 kV transmission line.

To calculate the propagation velocities at 25 kHz, enter the data shown in Fig. 31.

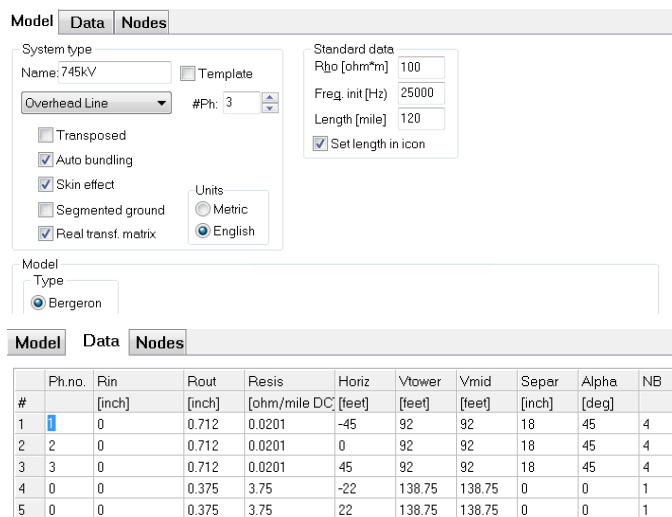


Fig. 31. LCC Program line data for calculating propagation velocity.

The LCC program provides the modal transformation matrix  $T_i$  and the propagation velocities for each mode (see

Table XIV and Table XV). We use this matrix to identify the modal information that the LCC program provides. We can recognize the modes in Table XIV as follows:

- The zero column has all values close to each other. This pattern indicates that all currents are flowing in the same direction.
- The beta column has two values close to each other with opposite sign and the remaining value close to zero. This pattern indicates that the current enters in one phase and returns in one of the other two phases.
- The alpha column has two values close to each other and the remaining value equal to their sum with opposite sign. This pattern indicates that the current enters in one phase and returns in the other two phases.

Knowing the modes, we can determine the velocities for each as shown in Table XV using the output data file with the LIS extension.

TABLE XIV  
 $T_i$  TRANSFORMATION MATRIX FOR 745 kV LINE EXAMPLE

	Zero (Mode 1)	Beta (Mode 2)	Alpha (Mode 3)
$T_i$	0.5985	-0.7071	-0.4086
	0.5325	0.0000	0.8161
	0.5985	0.7071	-0.4086

TABLE XV  
MODAL PROPAGATION VELOCITIES FOR 745 kV LINE EXAMPLE

Mode	Propagation Velocity	
	mi/s	pu of speed of light
Zero (1)	175,270.2	0.940884
Beta (2)	184,857.7	0.992352
Alpha (3)	186,160.2	0.999344

We recommend using the alpha mode propagation velocity to calculate the approximated value of the TWLPT setting, as follows.

$$TWLPT_{APPROX} = \frac{193.12 \text{ km}}{0.999344 \cdot 2.998 \cdot 10^8 \frac{\text{m}}{\text{s}}} = 644.59 \mu\text{s} \quad (114)$$

D. EMTP Modeling of Line Energization

A more accurate approach for estimating the TW line propagation time is to model the energization of the transmission line using an EMTP program. For this example, we use ATPDraw to model the 745 kV line. The model includes an additional line behind the line of interest to eliminate reflections from behind the relay location. All line sections use the J. Marti frequency-dependent model [9] to achieve more realistic results. Fig. 32 shows the one-line diagram of the test power system.

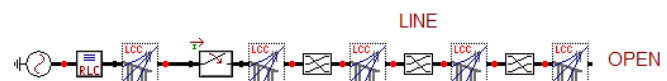


Fig. 32. ATPDraw power system model to simulate line energization.

We pass the primary currents through the differentiator-smoother described in [4] to extract the TWs from the phase currents and calculate the currents for the alpha mode. Fig. 33 shows the Alpha A current for the line energization case along with the wave arrival times. Using these times, we determine a TW line propagation delay of 647  $\mu$ s and a corresponding propagation velocity of 0.99564 pu. The difference between this propagation delay and the delay calculated in (114) is partly because the ATP line model accounts for the frequency spectrum of the TW and resulting distortion. The calculation in (114) uses a propagation velocity computed at a single frequency. Also, the value of 647  $\mu$ s is more appropriate as a setting than the value of 644.59  $\mu$ s, because it is derived using the same TW arrival time definition as the relay that uses the propagation time as a setting.

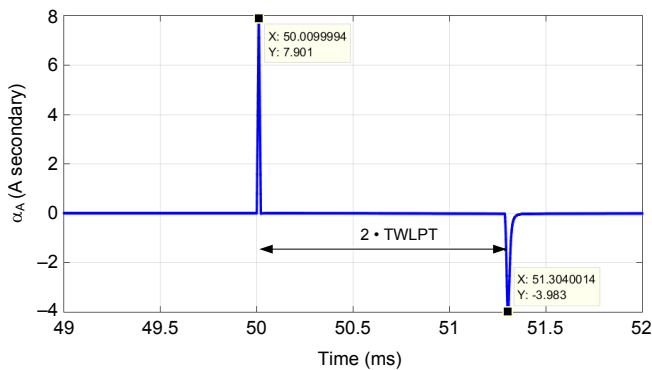


Fig. 33. Alpha A current during line energization and TW arrival times.

The calculations in this appendix provide an approximation of the TW line propagation time. In order to obtain the most accurate TW line propagation delay, the authors recommend performing the line energization test described in Section V, or monitoring the TWs at the line terminals for external events before selecting the TWLPT setting and enabling the TW87 scheme.

## XI. REFERENCES

- [1] E. O. Schweitzer, III, B. Kasztenny, A. Guzmán, V. Skendzic, and M. V. Mynam, "Speed of Line Protection – Can We Break Free of Phasor Limitations?" proceedings of the 41st Annual Western Protective Relay Conference, Spokane, WA, October 2014.
- [2] E. O. Schweitzer, III, B. Kasztenny, and M. V. Mynam, "Performance of Time-Domain Line Protection Elements on Real-World Faults," proceedings of the 42nd Annual Western Protective Relay Conference, Spokane, WA, October 2015.
- [3] E. O. Schweitzer, III, B. Kasztenny, M. V. Mynam, A. Guzmán, N. Fischer, and V. Skendzic, "Defining and Measuring the Performance of Line Protection Relays," proceedings of the 70th Annual Georgia Tech Protective Relaying Conference, April 2016.
- [4] E. O. Schweitzer, III, A. Guzmán, M. V. Mynam, V. Skendzic, B. Kasztenny, and S. Marx, "Locating Faults by the Traveling Waves They Launch," proceedings of the 40th Annual Western Protective Relay Conference, Spokane, WA, October 2013.
- [5] T. Liu and W. Scott-Meyer, *Electro-Magnetic Transients Program (EMTP) Theory Book*, Bonneville Power Administration, Portland, Oregon, June 1987.
- [6] L. M. Wedepohl, "Application of Matrix Methods to the Solution of Travelling Wave Phenomena in Polyphase Systems," proceedings of the IEE, Vol. 110, No. 12, December 1963, pp. 2200–2212.

- [7] D. E. Hedman, "Propagation on Overhead Transmission Lines I: Theory of Modal Analysis," *IEEE Transactions on Power Apparatus and Systems*, Vol. 84, Issue 3, March 1965, pp. 200–205.
- [8] E. Clarke, *Circuit Analysis of A-C Power Systems*. General Electric, Schenectady, NY, 1950.
- [9] J. R. Martí, "Accurate Modelling of Frequency-Dependent Transmission Lines in Electromagnetic Transient Simulations," *IEEE Transactions on Power Apparatus and Systems*, Vol. PAS-101, No. 1, January 1982, pp. 147–157.

## XII. BIOGRAPHIES

**Bogdan Kasztenny** is Senior Director, protection technology, in R&D at Schweitzer Engineering Laboratories, Inc. He has over 25 years of expertise in power system protection and control, including 10 years of academic career and 15 years of industrial experience, developing, promoting, and supporting many protection and control products. Bogdan is an IEEE Fellow, Senior Fulbright Fellow, Canadian representative of CIGRE Study Committee B5, registered professional engineer in the province of Ontario, and an adjunct professor at the University of Western Ontario. Bogdan serves on the Western Protective Relay Conference Program Committee (since 2011) and on the Developments in Power System Protection Conference Program Committee (since 2015). Bogdan has authored about 200 technical papers and holds 30 patents.

**Armando Guzmán** received his BSEE with honors from Guadalajara Autonomous University (UAG), Mexico. He received a diploma in fiber-optics engineering from Monterrey Institute of Technology and Advanced Studies (ITESM), Mexico, and his masters of science and PhD in electrical engineering and masters in computer engineering from the University of Idaho, USA. He served as regional supervisor of the Protection Department in the Western Transmission Region of the Federal Electricity Commission (the electrical utility company of Mexico) in Guadalajara, Mexico for 13 years. He lectured at UAG and the University of Idaho in power system protection and power system stability. Since 1993 he has been with Schweitzer Engineering Laboratories, Inc. in Pullman, Washington, where he is a fellow research engineer. He holds numerous patents in power system protection and metering. He is a senior member of IEEE.

**Normann Fischer** received a Higher Diploma in Technology, with honors, from Technikon Witwatersrand, Johannesburg, South Africa, in 1988; a BSEE, with honors, from the University of Cape Town in 1993; an MSEE from the University of Idaho in 2005; and a PhD from the University of Idaho in 2014. He joined Eskom as a protection technician in 1984 and was a senior design engineer in the Eskom protection design department for three years. He then joined IST Energy as a senior design engineer in 1996. In 1999, Normann joined Schweitzer Engineering Laboratories, Inc., where he is currently a fellow engineer in the research and development division. He was a registered professional engineer in South Africa and a member of the South African Institute of Electrical Engineers. He is currently a senior member of IEEE and a member of the American Society for Engineering Education (ASEE).

**Mangapathirao (Venkat) Mynam** received his MSEE from the University of Idaho in 2003 and his BE in electrical and electronics engineering from Andhra University College of Engineering, India, in 2000. He joined Schweitzer Engineering Laboratories, Inc. (SEL) in 2003 as an associate protection engineer in the engineering services division. He is presently working as a senior research engineer in SEL research and development. He was selected to participate in the U. S. National Academy of Engineering (NAE) 15th Annual U. S. Frontiers of Engineering Symposium. He is a senior member of IEEE and holds eight patents in the areas of power system protection, control, and fault location.

**Douglas Taylor** received his BSEE and MSEE degrees from the University of Idaho in 2007 and 2009, respectively. Since 2009, he has worked at Schweitzer Engineering Laboratories, Inc., and currently he is a lead research engineer in the research and development division. Mr. Taylor is a registered professional engineer in the state of Washington and is a member of the IEEE. His main interests are power system protection and power system analysis. He has authored several technical papers and holds one patent.